

Lepton flavor violating decays $Z \rightarrow l_i^\pm l_j^\mp$ in the B-L Supersymmetric Standard Model

Jia-Peng Huo^{1,2,3*}, Xing-Xing Dong^{1,2,3†}, Jiao Ma^{1,2,3‡}, Shu-Min Zhao^{1,2,3§},
Cai Guo^{1,2,3¶}, Hai-Bin Zhang^{1,2,3**}, Jin-Lei Yang^{1,2,3††}, Tai-Fu Feng^{1,2,3,4‡‡}

¹ *College of Physics Science and Technology,
Hebei University, Baoding, 071002, China*

² *Hebei Key Laboratory of High-precision Computation and
Application of Quantum Field Theory, Baoding, 071002, China*

³ *Hebei Research Center of the Basic Discipline
for Computational Physics, Baoding, 071002, China*

⁴ *Department of Physics, Chongqing University, Chongqing, 401331, China*

Abstract

Lepton flavor violation (LFV) represents a clear new physics (NP) signal beyond the standard model (SM). In this paper, we study LFV decays $Z \rightarrow l_i^\pm l_j^\mp$ in the B-L Supersymmetric Standard Model(B-LSSM). We calculate these processes separately in the mass eigenstate basis and the electroweak interaction basis, and the latter adopt the mass insertion approximation (MIA) method. The MIA clearly shows the effect of parameters on the LFV decays $Z \rightarrow l_i^\pm l_j^\mp$ in the analytic level, which provides a new way for us to analyze the LFV processes. At the same time, the corresponding constraints from the LFV decays $l_j^- \rightarrow l_i^- \gamma$ and $(g-2)_\mu$ are considered to analyze the numerical results.

PACS numbers: 11.30.Fs, 13.38.Dg, 14.60.-z

Keywords: Supersymmetry, Z boson decay, Lepton flavor violation

* qq2868371800@126.com

† dongxx@hbu.edu.cn

‡ majiaojiao65@126.com

§ zhaosm@hbu.edu.cn

¶ guocai0322@163.com

** hbzhang@hbu.edu.cn

†† jlyang@hbu.edu.cn

‡‡ fengtf@hbu.edu.cn

I. INTRODUCTION

In the SM, there are two different Yukawa matrices Y_u and Y_d in the quark sector, both involving the left-handed doublet Q_L of the quark field, which makes them impossible to diagonalize in the same basis at the same time[1]. This means that flavor violation exists in the quark sector and is controlled by the CKM matrix[2, 3]. The neutrinos have tiny masses and mix between generations[4, 5]. This indicates that lepton flavor is violated in the lepton sector. However, the SM cannot provide a reasonable explanation for either the small mass problem of neutrinos or the LFV. This suggests that the SM needs to be extended. Therefore the presence of any LFV signal may be regarded as evidence for the existence of NP beyond the SM[6].

In this work, we study the processes $Z \rightarrow l_i^\pm l_j^\mp$ in the B-LSSM[7–11], where B represents the baryon number and L stands for the lepton number. The B-LSSM is the $U(1)$ extension of Minimal Supersymmetric Standard Model(MSSM)[12–14], whose local gauge group is $SU(3)_C \otimes SU(2)_L \otimes U(1)_Y \otimes U(1)_{B-L}$. The right-handed neutrinos are introduced in this model, the conservation of lepton number is broken by making the neutrinos acquire mass through the seesaw mechanism. In this model, the invariance under $U(1)_{B-L}$ gauge group imposes the R-parity conservation[15].

These LFV processes $Z \rightarrow l_i^\pm l_j^\mp$ have been studied in many models[16–20], and most of these are studied in the mass eigenstate basis. This method depends on the transposed matrix, and it is difficult to see the effect of the parameters in the analytical level. To this end, we use a method called the MIA[21–24] to calculate these processes, which works directly on the mass matrix in the electroweak interaction basis instead of dealing with the mass matrix after the diagonalization in the physical basis. Compared with the mass eigenstate basis, the MIA provides a set of simple analytic formulas for the form factors. It can be emphasized which parameters will be effectively tested in the future colliders. In addition, the MIA provides the model-independent parameterization methods, which can be easily applied to the extended model of MSSM.

The paper is organized as follows. In Sec.II, we summarize the B-LSSM briefly, including its superpotential, the general soft SUSY-breaking terms and needed mass matrices. In Sec.III, we give the analytical expressions for $Z \rightarrow l_i^\pm l_j^\mp$ in the mass eigenstate basis and electroweak interaction basis, respectively. In Sec.IV, we give the numerical analysis. The

conclusion is discussed in Sec.V. The one-loop functions, the coupling coefficients in the mass eigenstate basis, the needed Feynman rules in the electroweak interaction basis, and the analytical expressions corresponding to Fig.2 and Fig.3 are collected in Appendix A, B, C and D, respectively.

II. THE B-LSSM

Compared with the MSSM, the B-LSSM adds two singlet Higgs superfields $\hat{\eta}$, $\hat{\bar{\eta}}$ and three generations of right-handed neutrinos superfields $\hat{\nu}_i^c$. The sneutrinos are disparted into CP-even sneutrinos and CP-odd sneutrinos, and their mass squared matrices are both extended to 6×6 .

In the TABLE I, we show the quantum numbers of gauge symmetry group for the chiral fields in the B-LSSM, the superpotential is given by

$$\begin{aligned}
W_{B-L} = & Y_{u,ij} \hat{Q}_i \hat{H}_u \hat{U}_j^c - Y_{d,ij} \hat{Q}_i \hat{H}_d \hat{D}_j^c + Y_{e,ij} \hat{L}_i \hat{H}_d \hat{R}_j + \mu_H \hat{H}_d \hat{H}_u \\
& + Y_{x,ij} \hat{\nu}_i^c \hat{\eta} \hat{\nu}_j^c + Y_{\nu,ij} \hat{L}_i \hat{H}_u \hat{\nu}_j^c - \mu_\eta \hat{\eta} \hat{\bar{\eta}},
\end{aligned} \tag{1}$$

where i, j represent the generation indices, $Y_{u,ij}, Y_{d,ij}, Y_{e,ij}, Y_{x,ij}$ and $Y_{\nu,ij}$ correspond to the Yukawa coupling coefficients. μ_H and μ_η are both the parameters with mass dimension. μ_H indicates the supersymmetric mass between $SU(2)_L$ Higgs doublets \hat{H}_d and \hat{H}_u , as well as μ_η represents the supersymmetric mass between $U(1)_{B-L}$ Higgs singlets $\hat{\eta}$ and $\hat{\bar{\eta}}$.

The $SU(2)_L \otimes U(1)_Y \otimes U(1)_{B-L}$ gauge group breaks to $U(1)_{em}$ as the Higgs fields obtain the vacuum expectation values (VEVs),

$$\begin{aligned}
H_d^0 &= \frac{1}{\sqrt{2}}(\phi_d + v_d + i\sigma_d), \quad H_u^0 = \frac{1}{\sqrt{2}}(\phi_u + v_u + i\sigma_u), \\
\eta &= \frac{1}{\sqrt{2}}(\phi_\eta + v_\eta + i\sigma_\eta), \quad \bar{\eta} = \frac{1}{\sqrt{2}}(\phi_{\bar{\eta}} + v_{\bar{\eta}} + i\sigma_{\bar{\eta}}),
\end{aligned} \tag{2}$$

where $\sigma_d, \sigma_u, \sigma_\eta, \sigma_{\bar{\eta}}$ represent the CP-odd Higgs components and $\phi_d, \phi_u, \phi_\eta, \phi_{\bar{\eta}}$ correspond to the CP-even Higgs components. The VEVs of the Higgs singlets $\hat{\eta}$ and $\hat{\bar{\eta}}$ satisfy $u = \sqrt{v_\eta^2 + v_{\bar{\eta}}^2}$. While the VEVs of the Higgs doublets \hat{H}_d and \hat{H}_u are v_d and v_u , which satisfy $v = \sqrt{v_d^2 + v_u^2}$. We take $\tan \beta' = \frac{v_{\bar{\eta}}}{v_\eta}$ by analogy to the definition $\tan \beta = \frac{v_u}{v_d}$ in the MSSM.

The $U(1)_{B-L}$ group introduces a new gauge field: B'^{BL} . The coupling between the gauge fields B'^{BL} and B^Y is given by the matrix $\begin{pmatrix} g_Y & g'_{YB} \\ g'_{BY} & g_{B-L} \end{pmatrix}$. With the condition of the two

TABLE I: The chiral superfields and quantum numbers in the B-LSSM.

Superfield	Spin 0	Spin $\frac{1}{2}$	Generations	$U(1)_Y \otimes SU(2)_L \otimes SU(3)_C \otimes U(1)_{B-L}$
\hat{H}_d	H_d	\tilde{H}_d	1	$(-\frac{1}{2}, \mathbf{2}, \mathbf{1}, 0)$
\hat{H}_u	H_u	\tilde{H}_u	1	$(\frac{1}{2}, \mathbf{2}, \mathbf{1}, 0)$
\hat{Q}_i	\tilde{Q}_i	Q_i	3	$(\frac{1}{6}, \mathbf{2}, \mathbf{3}, \frac{1}{6})$
\hat{L}_i	\tilde{L}_i	L_i	3	$(-\frac{1}{2}, \mathbf{2}, \mathbf{1}, -\frac{1}{2})$
\hat{D}_i^c	\tilde{D}_i^c	D_i^c	3	$(\frac{1}{3}, \mathbf{1}, \bar{\mathbf{3}}, -\frac{1}{6})$
\hat{U}_i^c	\tilde{U}_i^c	U_i^c	3	$(-\frac{2}{3}, \mathbf{1}, \bar{\mathbf{3}}, -\frac{1}{6})$
\hat{R}_i	\tilde{R}_i	R_i	3	$(1, \mathbf{1}, \mathbf{1}, \frac{1}{2})$
$\hat{\nu}_i^c$	$\tilde{\nu}_i^c$	ν_i^c	3	$(0, \mathbf{1}, \mathbf{1}, \frac{1}{2})$
$\hat{\eta}$	η	$\tilde{\eta}$	1	$(0, \mathbf{1}, \mathbf{1}, -1)$
$\hat{\bar{\eta}}$	$\bar{\eta}$	$\tilde{\bar{\eta}}$	1	$(0, \mathbf{1}, \mathbf{1}, 1)$

Abelian gauge groups unbroken, choosing matrix R in a proper form, one can write the coupling matrix as[7]

$$\begin{pmatrix} g_Y & g'_{YB} \\ g'_{BY} & g_{B-L} \end{pmatrix} R^T = \begin{pmatrix} g_1 & g_{YB} \\ 0 & g_B \end{pmatrix}, \quad (3)$$

and the transformation of the corresponding gauge field is

$$R \begin{pmatrix} B^Y \\ B'^{BL} \end{pmatrix} = \begin{pmatrix} B \\ B' \end{pmatrix}. \quad (4)$$

The two Abelian groups in the B-LSSM produce a new effect called as the gauge kinetic mixing. Due to the presence of the kinetic mixing terms, the B' boson mixes at tree level with the B and W^3 bosons. Basis on (B, W^3, B') , the mass matrix is

$$\begin{pmatrix} g_1^2 v^2 & -g_1 g_2 v^2 & g_1 g_{YB} v^2 \\ -g_1 g_2 v^2 & g_2^2 v^2 & -g_2 g_{YB} v^2 \\ g_1 g_{YB} v^2 & -g_2 g_{YB} v^2 & g_{YB}^2 v^2 + g_B^2 u^2 \end{pmatrix}. \quad (5)$$

This mass matrix can be diagonalized by a unitary matrix to get the physical mass eigen-

states γ , Z and Z' .

$$\begin{pmatrix} B \\ W \\ B' \end{pmatrix} = \begin{pmatrix} \cos \theta_W & \cos \theta'_W \sin \theta_W & -\sin \theta_W \sin \theta'_W \\ \sin \theta_W & -\cos \theta_W \cos \theta'_W & \cos \theta_W \sin \theta'_W \\ 0 & \sin \theta'_W & \cos \theta'_W \end{pmatrix} \begin{pmatrix} \gamma \\ Z \\ Z' \end{pmatrix}, \quad (6)$$

where θ_W and θ'_W are the corresponding Weinberg angles.

The soft breaking terms in the B-LSSM are written as

$$\begin{aligned} \mathcal{L}_{soft}^{B-L} = & -m_{\tilde{q},ij}^2 \tilde{Q}_i^* \tilde{Q}_j - m_{\tilde{u},ij}^2 \tilde{U}_i^* \tilde{U}_j - m_{\tilde{d},ij}^2 (\tilde{D}_i^c)^* \tilde{D}_j^c - m_{\tilde{L},ij}^2 \tilde{L}_i^* \tilde{L}_j - m_{\tilde{E},ij}^2 (\tilde{E}_i^c)^* \tilde{E}_j^c \\ & -m_{H_d}^2 |H_d|^2 - m_{H_u}^2 |H_u|^2 - m_\eta^2 |\eta|^2 - m_{\bar{\eta}}^2 |\bar{\eta}|^2 - m_{\tilde{\nu},ij}^2 (\tilde{\nu}_i^c)^* \tilde{\nu}_j^c + \left[-B_\mu H_d H_u \right. \\ & -B_\eta \eta \bar{\eta} + T_u^{ij} \tilde{Q}_i \tilde{U}_j^c H_u + T_d^{ij} \tilde{Q}_i \tilde{D}_j^c H_d + T_e^{ij} \tilde{L}_i \tilde{E}_j^c H_u + T_\nu^{ij} H_u \tilde{\nu}_i^c \tilde{L}_j + T_x^{ij} \eta \tilde{\nu}_i^c \tilde{\nu}_j^c \\ & \left. -\frac{1}{2}(M_1 \lambda_{\tilde{B}} \lambda_{\tilde{B}} + M_2 \lambda_{\tilde{W}} \lambda_{\tilde{W}} + M_3 \lambda_{\tilde{g}} \lambda_{\tilde{g}} + 2M_{BB'} \lambda_{\tilde{B}'} \lambda_{\tilde{B}} + M_{B'} \lambda_{\tilde{B}'} \lambda_{\tilde{B}'}) + h.c. \right], \quad (7) \end{aligned}$$

where $\lambda_{\tilde{B}}$, $\lambda_{\tilde{W}}$, $\lambda_{\tilde{g}}$ and $\lambda_{\tilde{B}'}$ are the gauginos of $U(1)_Y$, $SU(2)_L$, $SU(3)_C$ and $U(1)_{B-L}$ respectively. For the soft breaking slepton mass matrices $m_{L,\tilde{E}}^2$ and the trilinear coupling matrix T_e , we introduce the slepton flavor mixings, which take into account the off-diagonal terms[1, 18]

$$m_{\tilde{L}}^2 = \begin{pmatrix} m_L^2 & \delta_{12}^{LL} m_{LL}^2 & \delta_{13}^{LL} m_{LL}^2 \\ \delta_{12}^{LL} m_{LL}^2 & m_L^2 & \delta_{23}^{LL} m_{LL}^2 \\ \delta_{13}^{LL} m_{LL}^2 & \delta_{23}^{LL} m_{LL}^2 & m_L^2 \end{pmatrix}, \quad (8)$$

$$m_{\tilde{E}}^2 = \begin{pmatrix} m_E^2 & \delta_{12}^{RR} m_{EE}^2 & \delta_{13}^{RR} m_{EE}^2 \\ \delta_{12}^{RR} m_{EE}^2 & m_E^2 & \delta_{23}^{RR} m_{EE}^2 \\ \delta_{13}^{RR} m_{EE}^2 & \delta_{23}^{RR} m_{EE}^2 & m_E^2 \end{pmatrix}, \quad (9)$$

$$T_e = \begin{pmatrix} 1 & \delta_{12}^{LR} & \delta_{13}^{LR} \\ \delta_{12}^{LR} & 1 & \delta_{23}^{LR} \\ \delta_{13}^{LR} & \delta_{23}^{LR} & 1 \end{pmatrix} A_e. \quad (10)$$

The mass matrices we used can be obtained by SARAH[25]. We list some of these mass matrices here. In the B-LSSM, four 2-component spinors ($\lambda_{\tilde{W}}^-$, $\lambda_{\tilde{W}}^+$, \tilde{H}^- , \tilde{H}^+) form two four-component Dirac fermions (Charginos) χ^+ , χ^-

$$M_{\chi^\pm} = \begin{pmatrix} M_2 & \frac{1}{\sqrt{2}} g_2 v_u \\ \frac{1}{\sqrt{2}} g_2 v_d & \mu_H \end{pmatrix}. \quad (11)$$

This matrix is diagonalized by U and V :

$$U^* M_{\chi^\pm} V^\dagger = M_{\chi^\pm}^{\text{diag}}. \quad (12)$$

Based on $(\lambda_{\tilde{B}}, \lambda_{\tilde{W}}^3, \tilde{H}_d^0, \tilde{H}_u^0, \lambda_{\tilde{B}'}, \tilde{\eta}, \tilde{\bar{\eta}})$, seven Majorana fermions (Neutralinos) can be obtained:

$$M_{\chi^0} = \begin{pmatrix} M_1 & 0 & -\frac{1}{2}g_1 v_d & \frac{1}{2}g_1 v_u & M_{BB'} & 0 & 0 \\ 0 & M_2 & \frac{1}{2}g_2 v_d & -\frac{1}{2}g_2 v_u & 0 & 0 & 0 \\ -\frac{1}{2}g_1 v_d & \frac{1}{2}g_2 v_d & 0 & -\mu_H & -\frac{1}{2}g_{YB} v_d & 0 & 0 \\ \frac{1}{2}g_1 v_u & -\frac{1}{2}g_2 v_u & -\mu_H & 0 & \frac{1}{2}g_{YB} v_u & 0 & 0 \\ M_{BB'} & 0 & -\frac{1}{2}g_{YB} v_d & \frac{1}{2}g_{YB} v_u & M_{B'} & -g_B v_\eta & g_B v_{\bar{\eta}} \\ 0 & 0 & 0 & 0 & -g_B v_\eta & 0 & -\mu_\eta \\ 0 & 0 & 0 & 0 & g_B v_{\bar{\eta}} & -\mu_\eta & 0 \end{pmatrix}. \quad (13)$$

This matrix is diagonalized by N :

$$N^* M_{\chi^0} N^\dagger = M_{\chi^0}^{\text{diag}}. \quad (14)$$

Based on $(\tilde{L}_2^I, \tilde{R})$, the mass squared matrix for sleptons reads

$$\tilde{M}_l^2 = \begin{pmatrix} (M_L^2)_{LL} & (M_L^2)_{LR} \\ (M_L^2)_{LR}^\dagger & (M_L^2)_{RR} \end{pmatrix}, \quad (15)$$

$$\begin{aligned} (M_L^2)_{LL} &= m_L^2 + \mathbf{1} \frac{1}{8} ((g_1^2 + g_{YB}^2)(-v_u^2 + v_d^2) + g_2^2(-v_d^2 + v_u^2) + g_{YB} g_B (-2v_\eta^2 + 2v_{\bar{\eta}}^2 - v_d^2 + v_u^2) \\ &\quad + 2g_B^2(-v_\eta^2 + v_{\bar{\eta}}^2)) + \frac{1}{2} v_d^2 Y_e^\dagger Y_e, \\ (M_L^2)_{RR} &= m_E^2 + \mathbf{1} \frac{1}{8} (2(g_1^2 + g_{YB}^2)(-v_d^2 + v_u^2) - 2g_B^2(-v_\eta^2 + v_{\bar{\eta}}^2) + g_B g_{YB} (4v_\eta^2 - 4v_{\bar{\eta}}^2 - v_d^2 + v_u^2)) \\ &\quad + \frac{1}{2} v_d^2 Y_e Y_e^\dagger, \\ (M_L^2)_{LR} &= \frac{1}{\sqrt{2}} (v_d T_e^\dagger - v_u \mu Y_e^\dagger). \end{aligned} \quad (16)$$

This matrix is diagonalized by Z^E :

$$Z^E \tilde{M}_l^2 Z^{E,\dagger} = (M_l^2)^{\text{diag}}. \quad (17)$$

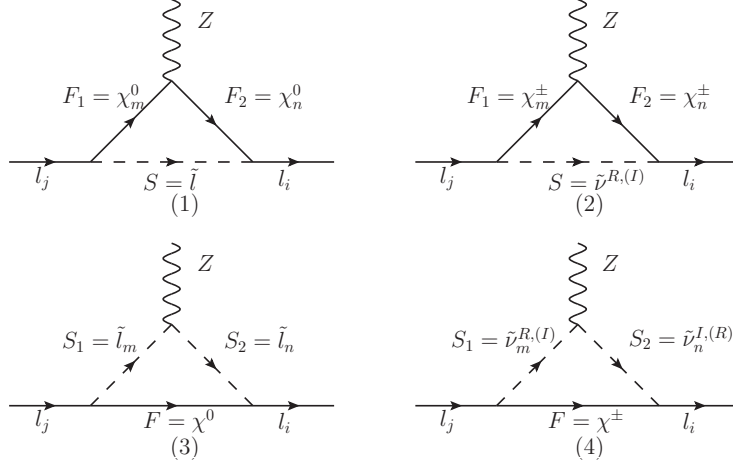


FIG. 1: Feynman diagrams for $Z \rightarrow l_i^\pm l_j^\mp$ in the mass eigenstate basis.

III. THE LFV DECAYS $Z \rightarrow l_i^\pm l_j^\mp$

The corresponding effective amplitude for $Z \rightarrow l_i^\pm l_j^\mp$, obtained through the effective Lagrangian, can be written as follows[26]:

$$\mathcal{M}(Z \rightarrow l_i^\pm l_j^\mp) = \bar{l}_i \gamma_\mu (A_L P_L + A_R P_R) l_j Z^\mu. \quad (18)$$

Then, we can obtain the branching ratios of $Z \rightarrow l_i^\pm l_j^\mp$:

$$Br(Z \rightarrow l_i^\pm l_j^\mp) = \frac{1}{12\pi} \frac{m_Z}{\Gamma_Z} (|A_L|^2 + |A_R|^2), \quad (19)$$

where Γ_Z denotes the total decay width of Z boson. In the numerical calculation, we choose $\Gamma_Z \simeq 2.4952 \text{ GeV}$ [27]. The coefficients $A_{L,R}$ can be obtained from the amplitudes of the Feynman diagrams.

A. The coefficients in the mass eigenstate basis

The corresponding Feynman diagrams for $Z \rightarrow l_i^\pm l_j^\mp$ are shown in Fig.1, where F and S represent Dirac (Majorana) fermions and scalar bosons, respectively. We then give specific

expressions for the coefficients of Eq.(18)

$$\begin{aligned}
A_L &= \frac{1}{2} \sum_{F=\chi^\pm, \chi^0} \sum_{S=\tilde{\nu}^{R,I}, \tilde{l}} \left[\frac{2m_{F_1} m_{F_2}}{\Lambda^2} H_R^{SF_2 l_i} H_L^{ZF_1 F_2} H_L^{S^* F_1 l_j} G_1(x_S, x_{F_1}, x_{F_2}) \right. \\
&\quad \left. - H_R^{SF_2 l_i} H_L^{ZF_2 F_1} H_L^{S^* F_1 l_j} G_2(x_S, x_{F_1}, x_{F_2}) \right] \\
&\quad - \frac{1}{2} \sum_{F=\chi^\pm, \chi^0} \sum_{S=\tilde{\nu}^{R,I}, \tilde{l}} \left[H_R^{FS_2 l_i} H_L^{ZS_2^* S_1} H_L^{S_1^* F l_j} G_2(x_F, x_{S_1}, x_{S_2}) \right], \\
A_R &= A_L|_{L \leftrightarrow R}.
\end{aligned} \tag{20}$$

Here, the concrete expressions for coupling coefficients $H_{L,R}$ and the one-loop functions can be found in Appendix A. Besides, we take $x = m^2/\Lambda^2$ with m being the mass of the corresponding particle, and Λ representing the energy scale of the NP.

B. The analytical results obtained through the MIA method

In contradistinction to the mass eigenstate basis, the Feynman diagrams of the MIA postulate that the external particles are assumed in the mass basis, whereas the internal sparticles operate within the electroweak interaction basis. The diagonal terms of the mass matrix are defined as the sparticle mass, and the off-diagonal terms are defined as the interaction vertices considered as mass insertions[28, 29]. The mass insertions can be categorized into two types: the flavor preservation and the flavor violation. The LFV comes from the off-diagonal terms of the sleptons (sneutrinos) mass matrix. Thus, we define ($i \neq j$)[1]

$$\Delta_{ij}^{LL} = (M_L^2)_{LL}^{ij} = (M_{\tilde{\nu}^{R,I}}^2)_{LL}^{ij}, \quad \Delta_{ij}^{LR} = (M_L^2)_{LR}^{ij}, \quad \Delta_{ij}^{RR} = (M_L^2)_{RR}^{ij}, \tag{21}$$

The terms L and R in Δ_{ij}^{AB} ($A, B = L, R$) specifically denote left-handed sleptons (sneutrinos) and right-handed sleptons. After our analysis, only these mass insertions change the flavor.

For the insertion of Δ_{ii}^{LR} , this case is considered an insertion that does not change flavor. Therefore, it is necessary to introduce an additional insert Δ_{ij}^{LL} or Δ_{ij}^{RR} ($i \neq j$) to change the flavor to meet the requirements.

The LFV processes in the MIA need to consider the trilinear couplings under the interaction eigenstate, so we show some couplings needed in this work as follows. The lepton-charginos-CP-even(odd) sneutrinos are deduced as:

$$\begin{aligned}
\mathcal{L}_{\tilde{l}_j \chi^- \tilde{\nu}^R} &= \frac{i}{\sqrt{2}} \bar{l}_j \tilde{\nu}_L^R [Y_l^j P_L \tilde{H}^- + g_2 P_R \lambda_{\tilde{W}}^-], \\
\mathcal{L}_{\tilde{l}_j \chi^- \tilde{\nu}^I} &= \frac{1}{\sqrt{2}} \bar{l}_j \tilde{\nu}_L^I [-Y_l^j P_L \tilde{H}^- + g_2 P_R \lambda_{\tilde{W}}^-].
\end{aligned} \tag{22}$$

The lepton-neutralinos-sleptons are deduced as:

$$\begin{aligned} \mathcal{L}_{\bar{l}_j \chi^0 \bar{l}} = & i\bar{l}_j \left\{ - \left[\frac{1}{\sqrt{2}} \left(2g_1 P_L \lambda_{\tilde{B}} + (g_B + 2g_{YB}) P_L \lambda_{\tilde{B}'} \right) \tilde{R} + Y_l^j P_L \tilde{H}_d^0 \tilde{L} \right] \right. \\ & \left. + \left[\frac{1}{\sqrt{2}} \left(g_2 P_R \lambda_{\tilde{W}}^3 + g_1 P_R \lambda_{\tilde{B}} + (g_B + g_{YB}) P_R \lambda_{\tilde{B}'} \right) \tilde{L} - Y_l^j P_R \tilde{H}_d^0 \tilde{R} \right] \right\}. \end{aligned} \quad (23)$$

We show Feynman diagrams using the MIA in Fig.2 and Fig.3. Here, $\tilde{S}_{1,2,3,4}$ is defined as $\lambda_{\tilde{B}}, \lambda_{\tilde{B}'}, \lambda_{\tilde{W}}^3, \tilde{H}^0$. m_{l_j} is the j-th generation lepton mass. \tilde{R}_i is the i-th generation right-handed slepton, \tilde{L}_i is the i-th generation left-handed slepton, $\tilde{\nu}_{L_j}^{R,I}$ is the j-th generation left-handed CP-even(odd) sneutrino. The Feynman diagrams including the right-handed sneutrino are strongly suppressed by the coupling parameter Y_ν , and the situations with right-handed sneutrino are neglected. To save space, we present the contributions from several special Feynman diagrams, the rest of which can be found in the Appendix D. The one-loop contributions from Fig.2(2a) are shown as:

$$\begin{aligned} A_L(2a) = & -\frac{1}{4\Lambda^2} g_2^3 \cos \theta \cos \theta' \Delta_{ij}^{LL} [G_3(x_2, x_{\tilde{\nu}_{L_j}^I}, x_{\tilde{\nu}_{L_i}^I}) - 2x_2 I_2(x_2, x_{\tilde{\nu}_{L_j}^I}, x_{\tilde{\nu}_{L_i}^I})] \\ & - \frac{1}{4\Lambda^2} g_2^3 \cos \theta \cos \theta' \Delta_{ij}^{LL} [G_3(x_2, x_{\tilde{\nu}_{L_j}^R}, x_{\tilde{\nu}_{L_i}^R}) - 2x_2 I_2(x_2, x_{\tilde{\nu}_{L_j}^R}, x_{\tilde{\nu}_{L_i}^R})]. \end{aligned} \quad (24)$$

The one-loop contributions from Fig.2(2b) are shown as:

$$\begin{aligned} A_R(2b) = & \frac{1}{2\Lambda^2} Y_{e,jj} Y_{e,ii} (-g_1 \sin \theta \cos \theta' + g_2 \cos \theta \cos \theta' + g_{YB} \sin \theta') \\ & \times \Delta_{ij}^{LL} [G_3(x_{\mu_H}, x_{\tilde{\nu}_{L_j}^I}, x_{\tilde{\nu}_{L_i}^I}) - 2x_2 I_2(x_{\mu_H}, x_{\tilde{\nu}_{L_j}^I}, x_{\tilde{\nu}_{L_i}^I})] \\ & + \frac{1}{2\Lambda^2} Y_{e,jj} Y_{e,ii} (-g_1 \sin \theta \cos \theta' + g_2 \cos \theta \cos \theta' + g_{YB} \sin \theta') \\ & \times \Delta_{ij}^{LL} [G_3(x_{\mu_H}, x_{\tilde{\nu}_{L_j}^R}, x_{\tilde{\nu}_{L_i}^R}) - 2x_2 I_2(x_{\mu_H}, x_{\tilde{\nu}_{L_j}^R}, x_{\tilde{\nu}_{L_i}^R})]. \end{aligned} \quad (25)$$

The one-loop contributions from Fig.2(4a) are shown as:

$$\begin{aligned} A_R(4a) = & -\frac{1}{8\Lambda^2} Y_{e,jj} Y_{e,ii} (g_2 \cos \theta \cos \theta' + g_2 \sin \theta \cos \theta' - (g_B + g_{YB}) \sin \theta') \\ & \times \Delta_{ij}^{LL} [G_3(x_{\tilde{\nu}_{L_j}^I}, x_{\tilde{\nu}_{L_i}^I}, x_{\mu_H}) + G_3(x_{\tilde{\nu}_{L_i}^I}, x_{\tilde{\nu}_{L_j}^I}, x_{\mu_H})] \\ & - \frac{1}{8\Lambda^2} Y_{e,jj} Y_{e,ii} (g_2 \cos \theta \cos \theta' + g_2 \sin \theta \cos \theta' - (g_B + g_{YB}) \sin \theta') \\ & \times \Delta_{ij}^{LL} [G_3(x_{\tilde{\nu}_{L_j}^R}, x_{\tilde{\nu}_{L_i}^R}, x_{\mu_H}) + G_3(x_{\tilde{\nu}_{L_i}^R}, x_{\tilde{\nu}_{L_j}^R}, x_{\mu_H})], \end{aligned} \quad (26)$$

$$\begin{aligned} A_L(4a) = & -\frac{1}{8\Lambda^2} g_2^2 (g_2 \cos \theta \cos \theta' + g_1 \sin \theta \cos \theta' - (g_B + g_{YB}) \sin \theta') \\ & \times \Delta_{ij}^{LL} [G_3(x_{\tilde{\nu}_{L_j}^I}, x_{\tilde{\nu}_{L_i}^I}, x_2) + G_3(x_{\tilde{\nu}_{L_i}^I}, x_{\tilde{\nu}_{L_j}^I}, x_2)] \\ & - \frac{1}{8\Lambda^2} g_2^2 (g_2 \cos \theta \cos \theta' + g_1 \sin \theta \cos \theta' - (g_B + g_{YB}) \sin \theta') \\ & \times \Delta_{ij}^{LL} [G_3(x_{\tilde{\nu}_{L_j}^R}, x_{\tilde{\nu}_{L_i}^R}, x_2) + G_3(x_{\tilde{\nu}_{L_i}^R}, x_{\tilde{\nu}_{L_j}^R}, x_2)]. \end{aligned} \quad (27)$$

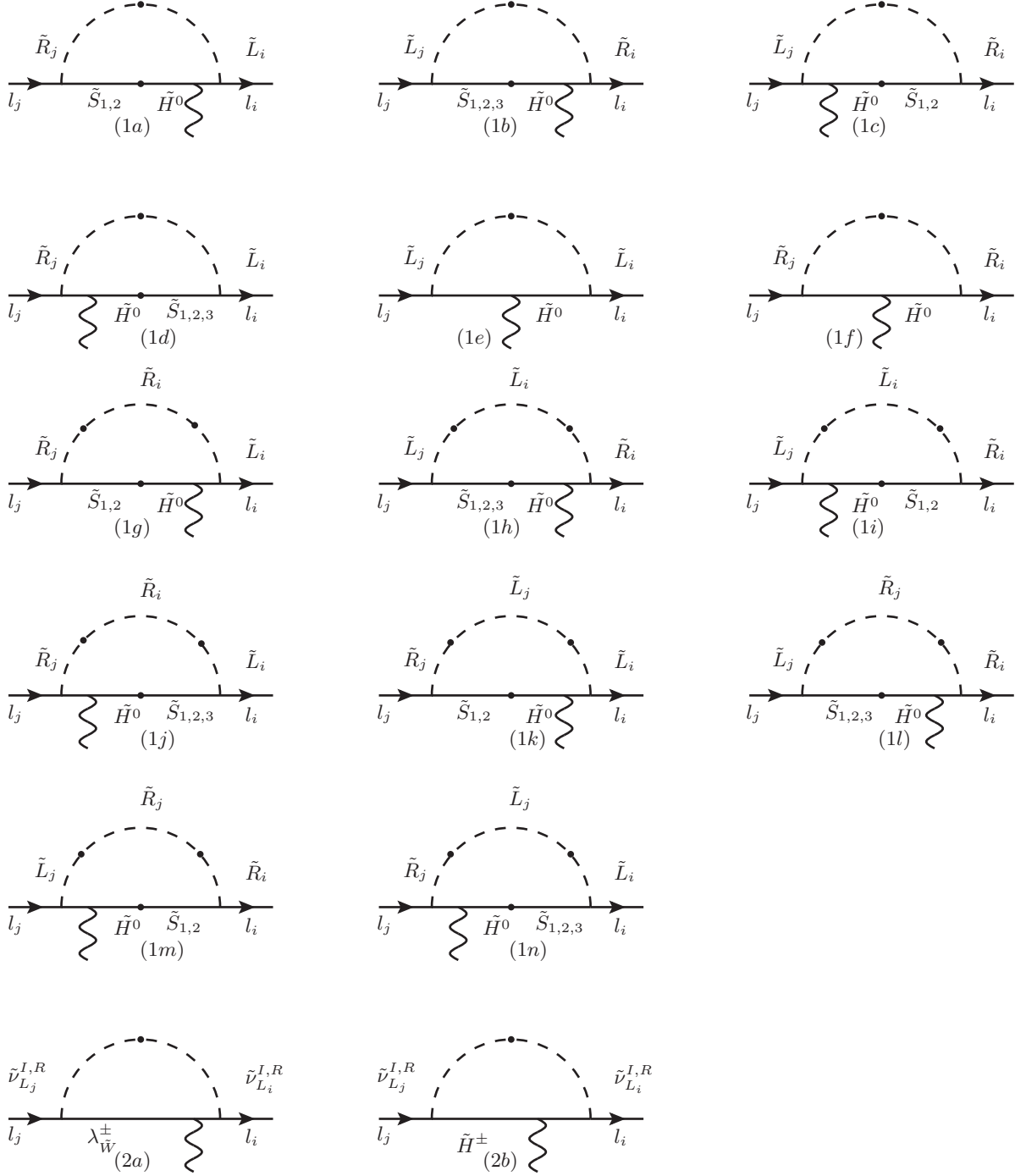


FIG. 2: The Feynman diagrams for $Z \rightarrow l_i^+ l_j^-$ in the electroweak interaction basis.

In these equations, the contributions from the parameters to the LFV process can be clearly seen. Especially, we can find that the contributions corresponding to Eq.(24)-Eq.(27) depend on the parameter Δ_{ij}^{LL} . Besides, from the equations listed in Appendix D, it follows that the one-loop contributions from Fig.2 and Fig.3 are affected by Δ_{ij}^{AB} ($A, B = L, R$). Consider

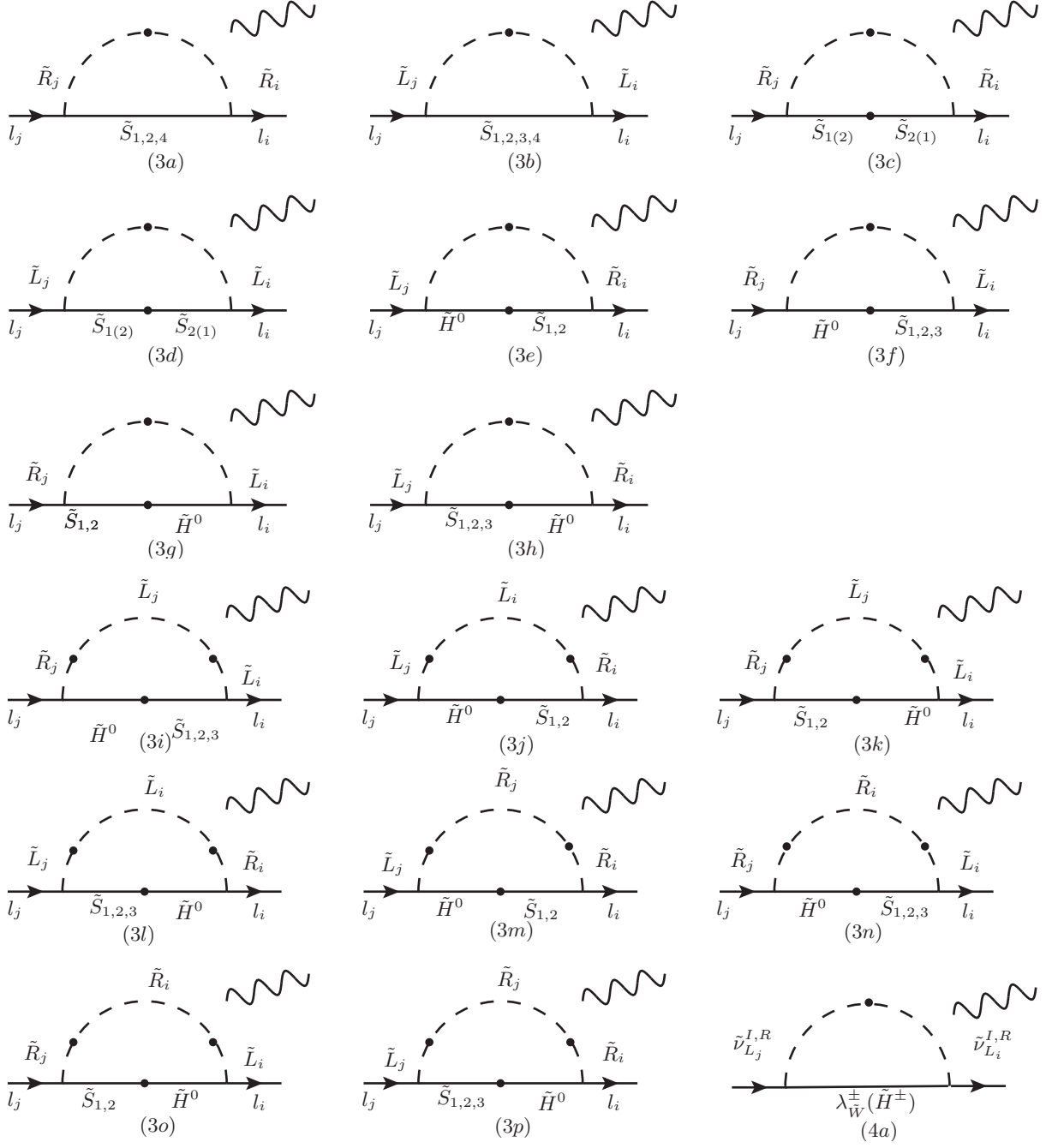


FIG. 3: The Feynman diagrams for $Z \rightarrow l_i^\pm l_j^\mp$ in the electroweak interaction basis.

the limiting case: $\Delta_{ij}^{AB} (A, B = L, R) = 0$, then $Br(Z \rightarrow l_i^\pm l_j^\mp) = 0$.

In order to more intuitively analyze the factors that affect LFV processes $Z \rightarrow l_i^\pm l_j^\mp$, we suppose that the sparticle masses are degenerate. In other words, we give the one-loop results in the extreme case where the sparticle masses and mass insertion treams are equal

to Λ :

$$\begin{aligned} M_1 = M_2 = \mu_H = M_{B'} = m_L = m_E = \tilde{M}_{\tilde{l},\tilde{\nu},ii} = \Lambda, \\ M_{BB'} = m_{LL} = m_{EE} = A_e = \Lambda. \end{aligned} \quad (28)$$

In this extreme degeneracy case, the corresponding one-loop functions in the electroweak interaction basis are subjected to limit operations, which are equal to some specific values:

$$\begin{aligned} G_3(1, 1, 1) = \frac{1}{48\pi^2}, \quad I_2(1, 1, 1) = -\frac{1}{96\pi^2}, \\ G_4(1, 1, 1, 1) = \frac{1}{192\pi^2}, \quad G_5(1, 1, 1, 1) = -\frac{1}{192\pi^2}. \end{aligned} \quad (29)$$

And mass insertions $\Delta_{ij}^{AB}(A, B = L, R)$ that change leptons flavor become the product of Λ^2 and the dimensionless parameters $\delta_{ij}^{AB}(A, B = L, R)$:

$$\Delta_{ij}^{LL} \approx \Lambda^2 \delta_{ij}^{LL}, \quad \Delta_{ij}^{LR} \approx \Lambda^2 \delta_{ij}^{LR}, \quad \Delta_{ij}^{RR} \approx \Lambda^2 \delta_{ij}^{RR}. \quad (30)$$

Then, we use these results to simplify all obtained coefficients to get some approximate results:

$$\begin{aligned} A_R^{\delta_{ij}^{RR}} &\approx \frac{1}{48\pi^2} C_R [g_1^2 + (g_B + 2g_{YB})^2], \\ A_L^{\delta_{ij}^{RR}} &\approx \frac{1}{48\pi^2} C_R g_1 (g_B + 2g_{YB}), \\ A_L^{\delta_{ij}^{LL}} &\approx -\frac{1}{12\pi^2} C_L [g_1^2 + (g_B + g_{YB})^2 + g_2^2] - \frac{1}{384\pi^2} C_L g_1 (g_B + g_{YB}) \\ &\quad - \frac{1}{24\pi^2} g_2^2 [g_2 \cos \theta \cos \theta' + g_1 \sin \theta \cos \theta' - (g_B + g_{YB}) \sin \theta'] \\ &\quad - \frac{1}{48\pi^2} g_2^3 \cos \theta \cos \theta', \\ A_R^{\delta_{ij}^{LR}} &\approx \frac{1}{192\pi^2} \times \frac{m_{l_i} + m_{l_j}}{8\Lambda} \tan \beta (C_L - C_R - 2E) [2g_1^2 + g_{YB} (g_B + 2g_{YB})], \\ A_L^{\delta_{ij}^{LR}} &\approx \frac{1}{192\pi^2} \times \frac{m_{l_i} + m_{l_j}}{8\Lambda} \tan \beta (C_R - C_L - 2E) [g_1^2 + g_{YB} (g_B + 2g_{YB}) - g_2^2]. \end{aligned} \quad (31)$$

Here, the coefficients C_L , C_R and E are collected in the Appendix D. By looking at these equations, we see that $\frac{m_{l_i} + m_{l_j}}{\Lambda} \ll 1$ in $A_{L,R}^{\delta_{ij}^{LR}}$, which lead to the numerical results of $A_{L,R}^{\delta_{ij}^{LR}}$ being much smaller than that of $A_{L,R}^{\delta_{ij}^{RR}}$ and $A_L^{\delta_{ij}^{LL}}$. This point will be confirmed in the numerical results of Section IV. In addition, we also see that parameter $\tan \beta$ is only coupled with $A_{L,R}^{\delta_{ij}^{LR}}$ in Eqs.(31), and the numerical results of $A_{L,R}^{\delta_{ij}^{LR}}$ analyzed above are very small, so the influence of $\tan \beta$ on $Z \rightarrow l_i^\pm l_j^\mp$ can be ignored.

IV. THE NUMERICAL ANALYSIS

In this section, we give the numerical analysis. In the B-LSSM, the $(g-2)_\mu$ and $l_j^- \rightarrow l_i^- \gamma$ have been discussed in Refs[30, 31], these two papers discuss the influence of sensitive parameters on $(g-2)_\mu$ and $l_j^- \rightarrow l_i^- \gamma$ under the mass eigenstates basis and the electroweak interaction basis. Consider the constraints of $(g-2)_\mu$ and $l_j^- \rightarrow l_i^- \gamma$, we restudy the Z boson decays $Z \rightarrow l_i^\pm l_j^\mp$.

The updated experimental data on the mass of Z' boson indicates $M'_Z > 5.1$ TeV with 95% confidence level (C.L.)[32], we choose $M'_Z = 5.4$ TeV in the following. Refs [33, 34] give an upper bound on the ratio between the Z' mass and its gauge coupling at 99% C.L. As $M'_Z/g_B \geq 6$ TeV, the scope of g_B is $0 < g_B \lesssim 0.9$. The LHC experimental data constrains $\tan \beta' < 1.5$ [35]. The coupling parameter g_{YB} will be taken around $-0.45 < g_{YB} < -0.05$ [7]. The large $\tan \beta$ has been excluded by the $\bar{B} \rightarrow X_s \gamma$ experiment[36, 37]. We select the suitable parameters, which are chosen as below:

$$\begin{aligned} M_1 &= 0.6\text{TeV}, A_e = 0.5\text{TeV}, \Lambda = 0.95\text{TeV}, M_2 = 0.7\text{TeV}, M_{BB'} = 0.8\text{TeV}, \\ g_{YB} &= -0.3, g_B = 0.6, \tan \beta = 20, \tan \beta' = 1.15, \mu_H = 0.85\text{TeV}, \\ m_L &= m_E = 1.2\text{TeV}, m_{EE} = m_{LL} = 1\text{TeV}. \end{aligned} \quad (32)$$

A. Constraints on $(g-2)_\mu$ and $l_j^- \rightarrow l_i^- \gamma$

The new experimental average for the difference between the experimental measurement and SM theoretical prediction of $(g-2)_\mu$ is given by[38]

$$\Delta a_\mu = a_\mu^{exp} - a_\mu^{SM} = (25.1 \pm 5.9) \times 10^{-10}. \quad (33)$$

In Fig.4, we show Δa_μ^{NP} versus $g_B, g_{YB}, \tan \beta, m_L, m_E$ and $\tan \beta'$. Under the 2σ limitation, the parameters g_B, g_{YB} and m_E are not sensitive to change. In addition, $m_L, \tan \beta$ and $\tan \beta'$ obtain reasonable parameter spaces, which are constrained as: $\tan \beta < 35, 0.9\text{TeV} < m_L < 1.7\text{TeV}, \tan \beta' < 1.4$.

After considering the constraints of $(g-2)_\mu$, we proceed to analyze the process of $\mu \rightarrow e\gamma$. The latest experimental datas for the CLFV processes $l_j^- \rightarrow l_i^- \gamma$ at 90% C.L. are [39, 40]

$$Br(\mu \rightarrow e\gamma) < 4.2 \times 10^{-13}, Br(\tau \rightarrow e\gamma) < 5.6 \times 10^{-8}, Br(\tau \rightarrow \mu\gamma) < 4.2 \times 10^{-8}. \quad (34)$$

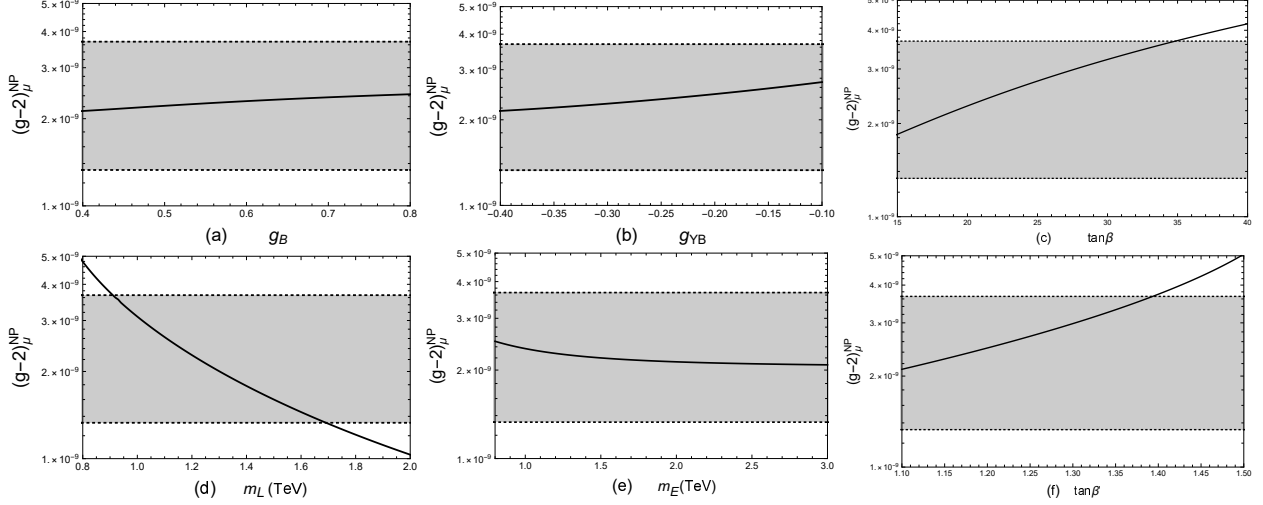


FIG. 4: Δa_μ^{NP} versus g_B , g_{YB} , $\tan\beta$, m_L , m_E and $\tan\beta'$, the gray area denotes the experimental 2σ interval.

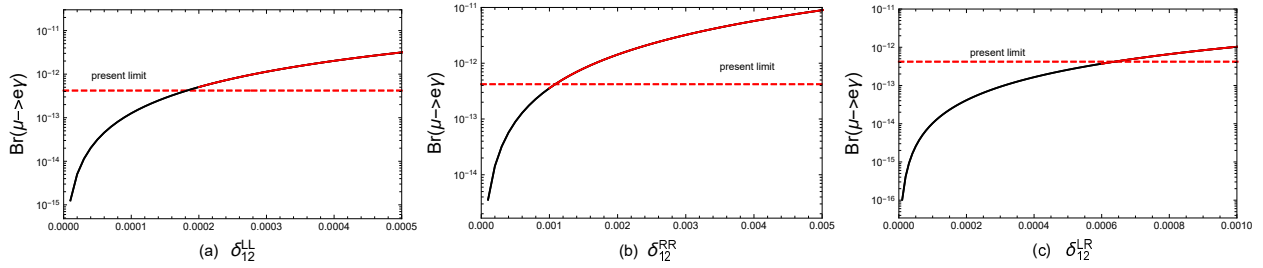


FIG. 5: The LFV rates for $\mu \rightarrow e\gamma$ versus δ_{ij}^{AB} , where the dashed red line denotes the present limit.

In Fig.5, we plot the LFV rates for $l_j^- \rightarrow l_i^- \gamma$ versus δ_{ij}^{AB} ($A, B = L, R$). The branching ratios increase with the increase of the parameters δ_{ij}^{AB} and reach the present limit. It can be seen that the parameters are constrained by the present limit:

$$\delta_{12}^{LL} < 0.0002, \quad \delta_{12}^{RR} < 0.001, \quad \delta_{12}^{LR} < 0.0006. \quad (35)$$

In Fig.6, we study the LFV rates for $\mu \rightarrow e\gamma$ versus m_L , m_E , m_{LL} and m_{EE} . In Fig.6 (a) and (c), we set $\delta_{12}^{RR} = \delta_{12}^{LR} = 0$, $\delta_{12}^{LL} = 0.0001$. Besides, parameters m_L , m_E , m_{LL} and m_{EE} undergo significant variations. It can be seen that the parameters (m_L , m_E) located in the diagonal elements of the slepton(sneutrino) mass matrix depress $Br(\mu \rightarrow e\gamma)$, and the off-diagonal elements (m_{LL} , m_{EE}) produce positive effects on $Br(\mu \rightarrow e\gamma)$. The parameters

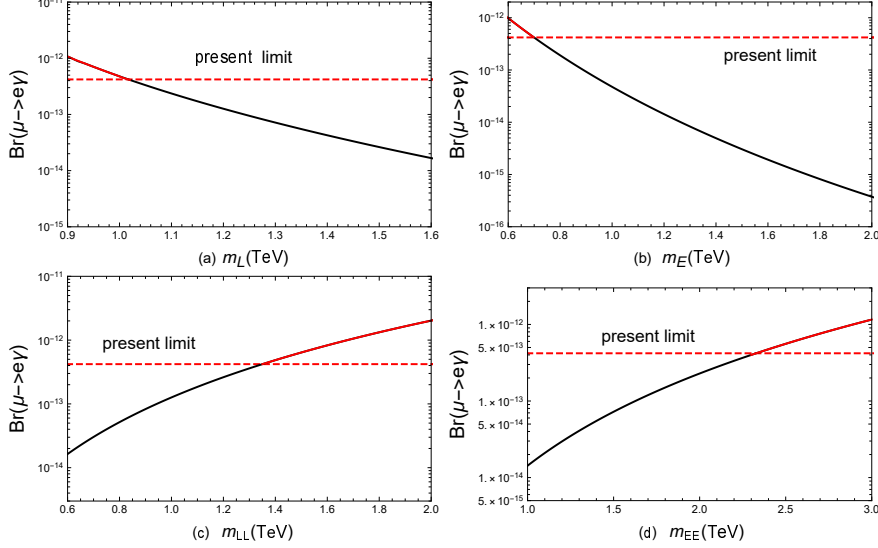


FIG. 6: The LFV rates for $\mu \rightarrow e\gamma$ versus M_L , M_E , M_{LL} and M_{EE} , where the dashed red line denotes the present limit.

are constrained by the present limit:

$$m_L > 1.05\text{TeV}, m_E > 0.7\text{TeV}, m_{LL} < 1.35\text{TeV}, m_{EE} < 2.3\text{TeV}. \quad (36)$$

Above all, we find that $\mu \rightarrow e\gamma$ has strict experimental constraints, which cause the parameters δ_{ij}^{AB} ($A, B = L, R$), m_L , m_E , m_{LL} and m_{EE} to be strictly affected. On this basis, we restudy the processes $Z \rightarrow l_i^\pm l_j^\mp$.

B. $Z \rightarrow l_i^\pm l_j^\mp$

The latest upper limits on the LFV branching ratio of $Z \rightarrow e\mu$, $Z \rightarrow e\tau$ and $Z \rightarrow \mu\tau$ at 95% C.L. are [41, 42]:

$$Br(Z \rightarrow e\mu) < 2.62 \times 10^{-7}, \quad Br(Z \rightarrow e\tau) < 5.0 \times 10^{-6}, \quad Br(Z \rightarrow \mu\tau) < 6.5 \times 10^{-6}. \quad (37)$$

Under the constraints of $(g-2)_\mu$ and $l_j^- \rightarrow l_i^- \gamma$, we research the branching ratios of the LFV processes $Z \rightarrow l_i^\pm l_j^\mp$.

1. $Z \rightarrow e\mu$

In general, the non-diagonal elements of the slepton (sneutrino) mass matrix are considered to be the origin of flavor violation[1]. In Fig.7, we plot the contributions from the LFV

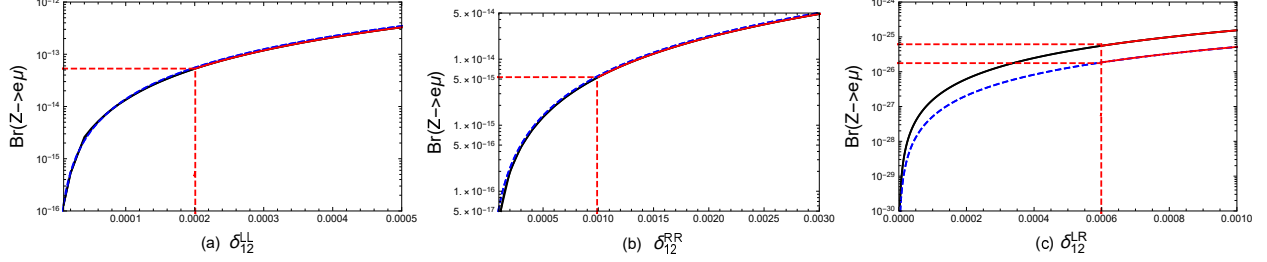


FIG. 7: The LFV rates for $Z \rightarrow e\mu$ versus δ_{12}^{LL} , δ_{12}^{RR} , δ_{12}^{LR} , where the solid black line represents the results in the mass eigenstate basis, the dashed blue line represents the results in the electroweak interaction basis. The red solid line is consistent with the present limit of $l_j^- \rightarrow l_i^- \gamma$.

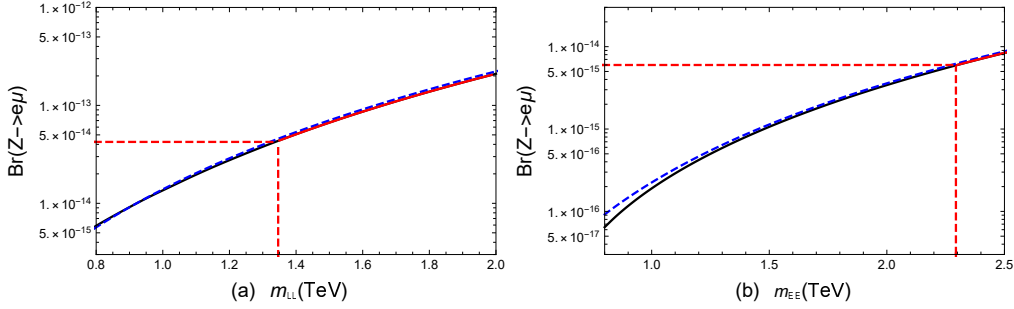


FIG. 8: The LFV rates for $Z \rightarrow e\mu$ versus m_{LL} and m_{EE} , where the solid black line represents the results in the mass eigenstate basis, the dashed blue line represents the results in the electroweak interaction basis. The red solid line is consistent with the present limit of $l_j^- \rightarrow l_i^- \gamma$.

process $Z \rightarrow e\mu$ changing with the parameters δ_{12}^{LL} , δ_{12}^{RR} and δ_{12}^{LR} individually. By comparing the calculation results of the two methods, it can be concluded that the results from parameters δ_{12}^{LL} and δ_{12}^{RR} are similarly the same, while the difference from parameter δ_{12}^{LR} in two methods is about one order. However, due to the small contribution from parameter δ_{12}^{LR} , this difference can be ignored. Comparing these three parameters, we find that the effect from δ_{12}^{LR} is much smaller than that of δ_{12}^{RR} and δ_{12}^{LL} , which can confirm the result obtained by approximating analysis in Section III. We can see that the main contributions calculated in two different eigenstates are very similar, and the accuracy of the MIA results is verified. Besides, it can be observed that the branching ratios increase obviously as parameters δ_{12}^{AB} ($A, B = L, R$) increase. Therefore, we deduce that parameters δ_{12}^{AB} ($A, B = L, R$) are sensitive parameters and have a strong effect on the LFV. The branching ratio $Br(Z \rightarrow e\mu)$ is lower than 10^{-13} due to the constraints of $l_j^- \rightarrow l_i^- \gamma$.

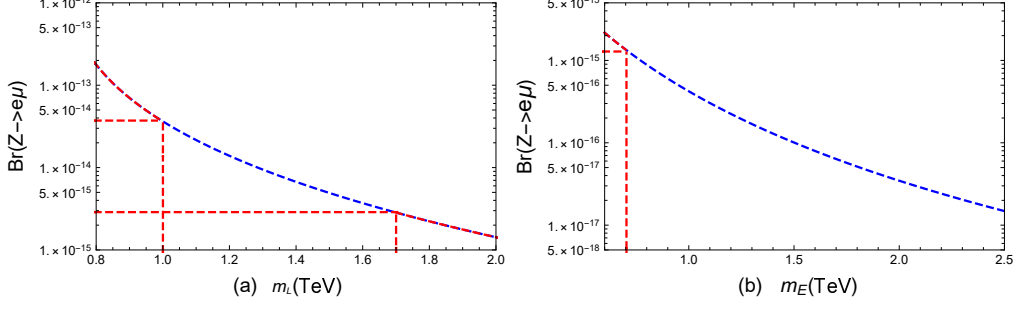


FIG. 9: The LFV rates for $Z \rightarrow e\mu$ versus m_L and m_E , where the dashed blue line represents the results in the electroweak interaction basis. The dashed red line indicates exclusion of $(g-2)_\mu$ or $l_j^- \rightarrow l_i^- \gamma$.

The parameters m_{LL} and m_{EE} located in the non-diagonal elements of slepton (sneutrino) matrices also have a large effect on the LFV. We show $Br(Z \rightarrow e\mu)$ versus m_{LL} and m_{EE} in the Fig.8. In Fig.8(a), we set $\delta_{12}^{RR} = \delta_{12}^{LR} = 0$, $\delta_{12}^{LL} = 0.0001$. In Fig.8(b), we set $\delta_{12}^{RR} = 0.0002$, $\delta_{12}^{LL} = \delta_{12}^{LR} = 0$. It can be observed that both parameters show clear trends and have a positive impact on the process $Z \rightarrow e\mu$. This indicates the parameters m_{LL} and m_{EE} enhance the LFV effect. Under the constraints of $l_j^- \rightarrow l_i^- \gamma$, the branching ratio can reach the order around 10^{-14} .

The parameters m_L and m_E , which exist in all one-loop functions in the electroweak interaction basis, are the diagonal elements of soft breaking slepton (sneutrino) mass matrices $m_{\bar{L},\bar{R}}^2$ and associated with the slepton (sneutrino) masses in the MIA. We set $\delta_{12}^{RR} = \delta_{12}^{LR} = 0$, $\delta_{12}^{LL} = 0.0001$ in Fig.9(a) and $\delta_{12}^{RR} = 0.0002$, $\delta_{12}^{LL} = \delta_{12}^{LR} = 0$ in Fig.9(b), and study the branching ratios of $Z \rightarrow e\mu$ changing with m_L and m_E , respectively. The numerical results indicate that when parameter m_L or m_E increase, the branching ratio decreases. This indicates the diagonal elements of the slepton (sneutrinos) matrices suppress the LFV effect. The numerical results also show that the contribution of $Br(Z \rightarrow e\mu)$ changing with parameter m_L is limited to $10^{-15} \sim 10^{-14}$ under the constraints of $(g-2)_\mu$ or $l_j^- \rightarrow l_i^- \gamma$, while the contribution of parameter m_E is less than 10^{-15} under the constraints of $l_j^- \rightarrow l_i^- \gamma$.

2. $Z \rightarrow e\tau$ and $Z \rightarrow \mu\tau$

In this subsection, we study the LFV processes $Z \rightarrow e\tau$ and $Z \rightarrow \mu\tau$, as detailed in FIG.10, FIG.11 and FIG.12. The numerical results show that the diagonal elements(m_E ,

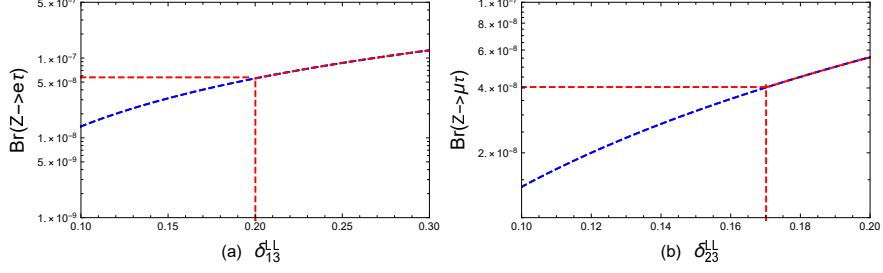


FIG. 10: The LFV rates for $Z \rightarrow e\tau$ and $Z \rightarrow \mu\tau$ versus δ_{13}^{LL} , δ_{23}^{LL} . The dashed red line indicates exclusion by $l_j^- \rightarrow l_i^- \gamma$.

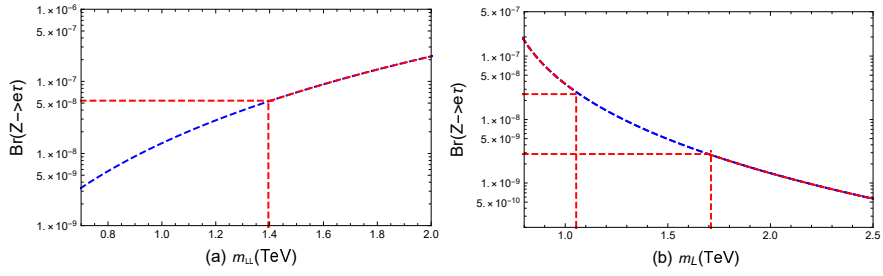


FIG. 11: Taking $\delta_{13}^{LL} = 0.1$, $\delta_{13}^{LR} = \delta_{13}^{RR} = 0$, we plot the LFV rates for $Z \rightarrow e\tau$ versus m_{LL} and m_L , where the dashed blue line represents the results in the electroweak interaction basis. The dashed red line indicates exclusion of $\tau \rightarrow e\gamma$.

m_L) of the slepton(sneutrino) mass matrix increase the LFV effect, while off-diagonal elements (δ_{13}^{LL} , δ_{23}^{LL} , m_{EE} , m_{LL}) decrease the LFV effect. In FIG.10, we plot the $Br(Z \rightarrow e\tau)$ and $Br(Z \rightarrow \mu\tau)$ versus parameters δ_{13}^{LL} and δ_{23}^{LL} . Under the present limits of $l_j^- \rightarrow l_i^- \gamma$, the parameters δ_{13}^{LL} and δ_{23}^{LL} are respectively limited to: $\delta_{13}^{LL} < 0.2$, $\delta_{23}^{LL} < 0.17$, and $Br(Z \rightarrow e\tau)$ and $Br(Z \rightarrow \mu\tau)$ can be both approximate to 10^{-8} . As $\delta_{13}^{LL} = 0.1$, $\delta_{23}^{RR} = 0.3$, we study the $Br(Z \rightarrow e\tau)$ and $Br(Z \rightarrow \mu\tau)$ changing with parameters m_{LL} , m_L , m_{EE} and m_E in Fig.11 and Fig.12. Under the present limits of $l_j^- \rightarrow l_i^- \gamma$ and $(g-2)_\mu$, the branching ratios of $Z \rightarrow e\tau$ and $Z \rightarrow \mu\tau$ can be in the order around 5×10^{-8} . In particular, the value of parameter m_L is constrained to be between 1TeV and 1.7TeV, and the $Br(Z \rightarrow e\tau)$ is corresponding in the range of $3 \times 10^{-9} \sim 5 \times 10^{-8}$.

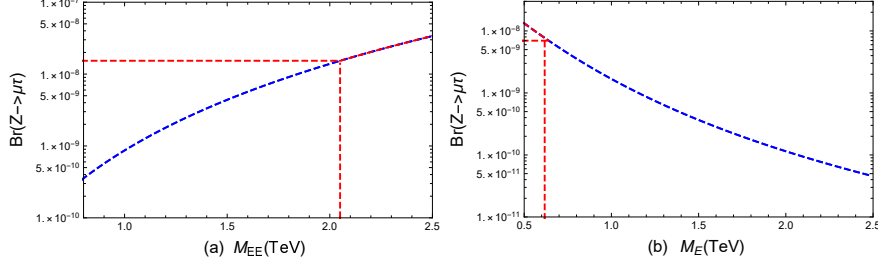


FIG. 12: Taking $\delta_{23}^{RR} = 0.3$, $\delta_{23}^{LR} = \delta_{23}^{LL} = 0$, we show the LFV rates for $Z \rightarrow \mu\tau$ versus m_{EE} and m_E , where the dashed blue line represents the results in the electroweak interaction basis. The dashed red line indicates exclusion of $\tau \rightarrow \mu\gamma$.

V. DISCUSSION AND CONCLUSION

In this paper, we study the LFV process $Z \rightarrow l_i^\pm l_j^\mp$ in the B-LSSM. We calculate this process in the mass eigenstate basis and the electroweak interaction basis, respectively. Comparing the results obtained by the two methods, the two curves have the same change trends and the corresponding main contributions are almost in the same order. The advantageous aspect of the MIA lies in its ability to reveal the functional correlation between the parameter and the associated branching ratio at the analytical level. When we analyze a certain parameter, the function of the branching ratio changing with the parameter can be precisely found out easily by their analytical equations.

We find that the parameters δ_{ij}^{AB} ($A, B = L, R$), m_L , m_E , m_{EE} and m_{LL} in the slepton (sneutrino) mass matrix have a significant effect on the $Br(Z \rightarrow l_i^\pm l_j^\mp)$. Here, δ_{12}^{AB} ($A, B = L, R$), m_{LL} and m_{EE} present in the off-diagonal of the slepton (sneutrinos) mass matrix, whose increase enlarge the branching ratios of $Z \rightarrow l_i^\pm l_j^\mp$. As the diagonal terms of slepton (sneutrino) mass matrix, the increase of m_L and m_E decrease the branching ratios of $Z \rightarrow l_i^\pm l_j^\mp$. Therefore, the diagonal elements of the slepton (sneutrino) mass matrix suppress the LFV effect, while the off-diagonal elements enhance the LFV effect. This property is similar to other LFV processes (e.g., $l_j^- \rightarrow l_i^- \gamma$).

Through the numerical analysis, we find that $(g-2)_\mu$ and $l_j^- \rightarrow l_i^- \gamma$ have certain constraints on the parameter spaces, and the parameters in the slepton (sneutrinos) mass matrix are the most stringent, such as parameters δ_{ij}^{AB} ($A, B = L, R$), m_{EE} , m_E , m_{LL} and m_L are constrained. Considering the constraints of $(g-2)_\mu$ and $l_j^- \rightarrow l_i^- \gamma$, the $Br(Z \rightarrow e\mu)$ can be in the order around 10^{-14} , and the upper bounds of $Br(Z \rightarrow e\tau)$ and $Br(Z \rightarrow \mu\tau)$ can reach

5×10^{-8} . More specifically, as the parameter m_L is restricted between 1TeV and 1.7TeV, the branching ratios of $Z \rightarrow l_i^\pm l_j^\mp$ that are strictly limited as: $3 \times 10^{-15} < Br(Z \rightarrow e\mu) < 4 \times 10^{-14}$ and $3 \times 10^{-9} < Br(Z \rightarrow e\tau) < 5 \times 10^{-8}$. The numerical results discussed above all satisfy the present constraints of $Z \rightarrow l_i^\pm l_j^\mp$. We hope that the experimental results for $Z \rightarrow l_i^\pm l_j^\mp$ can be detected in the future, which may provide the possibilities for finding NP beyond the SM.

Acknowledgments This work is supported by the Major Project of National Natural Science Foundation of China (NNSFC) (No. 12235008), the National Natural Science Foundation of China (NNSFC) (No. 12075074, No. 12075073), the Natural Science Foundation of Hebei province (No. A2022201022, No. A2020201002, No. A2023201041, No. A2022201017), the Natural Science Foundation of Hebei Education Department (No. QN2022173).

Appendix A: The one-loop functions

The one-loop functions $I_2(x, y, z)$, $G_1(x, y, z)$, $G_2(x, y, z)$, $G_3(x, y, z)$, $G_4(x, y, z, t)$, $G_5(x, y, z, t)$, $G_6(x, y, z, t, n)$ and $G_7(x, y, z, t, n)$ can be written as

$$\begin{aligned}
I_2(x, y, z) &= \frac{1}{16\pi^2} \left[\frac{1 + \ln x}{(z-x)(y-x)} - \frac{x \ln x}{(x-y)^2(x-z)} - \frac{x \ln x}{(x-z)^2(x-y)} \right. \\
&\quad \left. - \frac{y \ln y}{(x-y)^2(z-y)} - \frac{z \ln z}{(x-y)^2(y-z)} \right], \\
G_1(x, y, z) &= \frac{1}{16\pi^2} \left[\frac{x \ln x}{(z-x)(y-x)} + \frac{y \ln y}{(x-y)(z-y)} + \frac{z \ln z}{(x-z)(y-z)} \right], \\
G_2(x, y, z) &= \frac{1}{16\pi^2} \left[\frac{x^2 \ln x}{(z-x)(y-x)} + \frac{y^2 \ln y}{(x-y)(z-y)} + \frac{z^2 \ln z}{(x-z)(y-z)} \right], \\
G_3(x, y, z) &= \frac{1}{16\pi^2} \left[\frac{x + 2x \ln x}{(z-x)(y-x)} + \frac{x^2 \ln x}{(z-x)(y-x)^2} + \frac{x^2 \ln x}{(y-x)(z-x)^2} \right. \\
&\quad \left. + \frac{y^2 \ln y}{(y-z)(x-y)^2} + \frac{z^2 \ln z}{(y-z)(x-z)^2} \right], \\
G_4(x, y, z, t) &= \frac{1}{16\pi^2} \left[\frac{2x \ln x}{(x-y)(x-z)} - \frac{2x \ln x}{(x-t)(x-y)} - \frac{x^2 \ln x}{(x-z)(x-y)^2} + \frac{x^2 \ln x}{(x-t)(x-y)^2} \right. \\
&\quad - \frac{x^2 \ln x}{(x-y)(x-z)^2} + \frac{x^2 \ln x}{(x-y)(x-t)^2} - \frac{y^2 \ln y}{(z-y)(x-y)^2} + \frac{y^2 \ln y}{(t-y)(x-y)^2} \\
&\quad \left. - \frac{z^2 \ln z}{(y-z)(x-z)^2} + \frac{t^2 \ln t}{(y-t)(x-t)^2} \right] \frac{1}{z-t}, \\
G_5(x, y, z, t) &= \frac{1}{16\pi^2} \left[\frac{1 + \ln x}{(x-y)(x-z)} - \frac{1 + \ln x}{(x-t)(x-y)} - \frac{x \ln x}{(x-z)(x-y)^2} + \frac{x \ln x}{(x-t)(x-y)^2} \right. \\
&\quad - \frac{x \ln x}{(x-y)(x-z)^2} + \frac{x \ln x}{(x-y)(x-t)^2} - \frac{y \ln y}{(z-y)(x-y)^2} + \frac{y \ln y}{(t-y)(x-y)^2} \\
&\quad \left. - \frac{z \ln z}{(y-z)(x-z)^2} + \frac{t \ln t}{(y-t)(x-t)^2} \right] \frac{1}{z-t}, \\
G_6(x, y, z, t, n) &= [G_4(x, y, z, t) - G_4(x, y, z, n)] \frac{1}{t-n}, \\
G_7(x, y, z, t, n) &= [G_5(x, y, z, t) - G_5(x, y, z, n)] \frac{1}{t-n}.
\end{aligned}$$

Appendix B: The couplings in the mass eigenstate basis

$$\begin{aligned}
H_L^{Z\chi_i^0\chi_j^0} &= -\frac{i}{2}(N_{j,3}^*(g_1 \sin \theta_W \cos \theta'_W + g_2 \cos \theta_W \cos \theta'_W - g_{YB} \sin \theta'_W)N_{i,3} \\
&\quad - N_{j,4}^*(g_1 \sin \theta_W \cos \theta'_W + g_2 \cos \theta_W \cos \theta'_W - g_{YB} \sin \theta'_W)N_{i,4} \\
&\quad - 2g_B \sin \theta'_W(N_{j,6}^*N_{i,6} - N_{j,7}^*N_{i,7})) \\
H_R^{Z\chi_i^0\chi_j^0} &= \frac{i}{2}(N_{i,3}^*(g_1 \sin \theta_W \cos \theta'_W + g_2 \cos \theta_W \cos \theta'_W - g_{YB} \sin \theta'_W)N_{j,3} \\
&\quad - N_{i,4}^*(g_1 \sin \theta_W \cos \theta'_W + g_2 \cos \theta_W \cos \theta'_W - g_{YB} \sin \theta'_W)N_{j,4} \\
&\quad - 2g_B \sin \theta'_W(N_{i,6}^*N_{j,6} - N_{i,7}^*N_{j,7})) \\
H_L^{Z\chi_i^\pm\chi_j^\pm} &= \frac{i}{2}(2g_2U_{j,1}^* \cos \theta \cos \theta' U_{i,1} \\
&\quad + U_{j,2}^*(-g_1 \sin \theta \cos \theta' + g_2 \cos \theta \cos \theta' + g_{YB} \sin \theta')U_{i,2}) \\
H_R^{Z\chi_i^\pm\chi_j^\pm} &= \frac{i}{2}(2g_2V_{i,1}^* \cos \theta \cos \theta' V_{j,1} \\
&\quad + V_{i,2}^*(-g_1 \sin \theta \cos \theta' + g_2 \cos \theta \cos \theta' + g_{YB} \sin \theta')V_{j,2}) \\
H^{Z\tilde{\nu}_j^I\tilde{\nu}_j^R} &= \frac{1}{2}(g_1 \cos \theta' \sin \theta + g_2 \cos \theta \cos \theta' - (g_{YB} + g_B) \sin \theta') \sum_{j_1=1}^3 Z_{i,j_1}^{I,*} Z_{j,j_1}^{R,*} \\
&\quad - g_B \sin \theta' \sum_{j_1=1}^3 Z_{i,3+j_1}^{I,*} Z_{j,3+j_1}^{R,*} \\
H^{Z\tilde{l}_i\tilde{l}_j} &= \frac{i}{2}(-g_1 \sin \theta \cos \theta' + g_2 \cos \theta \cos \theta' + (g_{YB} + g_B) \sin \theta') \sum_{j_1=1}^3 Z_{i,j_1}^{E,*} Z_{j,j_1}^E \\
&\quad - (2g_1 \sin \theta \cos \theta' - (2g_{YB} + g_B) \sin \theta') \sum_{j_1=1}^3 Z_{i,3+j_1}^{E,*} Z_{j,3+j_1}^E \\
H_L^{l_j^I\tilde{l}_k\chi_i^0} &= \frac{i}{2}(\sqrt{2}g_1N_{i,1}^*Z_{k,j}^E + \sqrt{2}g_2N_{i,2}^*Z_{k,j}^E + \sqrt{2}g_{YB}N_{i,5}^*Z_{k,j}^E \\
&\quad + \sqrt{2}g_B N_{i,5}^*Z_{k,j}^E + 2N_{i,3}^*Y_{e,jj}Z_{k,3+j}^E) \\
H_R^{l_j^I\tilde{l}_k\chi_i^0} &= i(-\frac{1}{\sqrt{2}}Z_{k,3+j}^E(2g_1N_{i,1} + (2g_{YB} + g_B)N_{i,5}) - Y_{e,jj}^*Z_{k,j}^E N_{i,3}) \\
H_L^{l_j^I\tilde{\nu}_k\chi_i^\pm} &= \frac{1}{\sqrt{2}}(-g_2V_{i,1}^*Z_{k,j}^{I,*} + V_{i,2}^*Z_{k,3+j}^{I,*}Y_{\nu,jj}^*) \\
H_R^{l_j^I\tilde{\nu}_k\chi_i^\pm} &= \frac{1}{\sqrt{2}}(Z_{k,j}^{I,*}Y_{e,jj}^*U_{i,2}) \\
H_L^{l_j^R\tilde{\nu}_k\chi_i^\pm} &= i\frac{1}{\sqrt{2}}(-g_2V_{i,1}^*Z_{k,j}^{R,*} + V_{i,2}^*Z_{k,3+j}^{R,*}Y_{\nu,jj}^*) \\
H_R^{l_j^R\tilde{\nu}_k\chi_i^\pm} &= i\frac{1}{\sqrt{2}}(Z_{k,j}^{R,*}Y_{e,jj}^*U_{i,2})
\end{aligned}$$

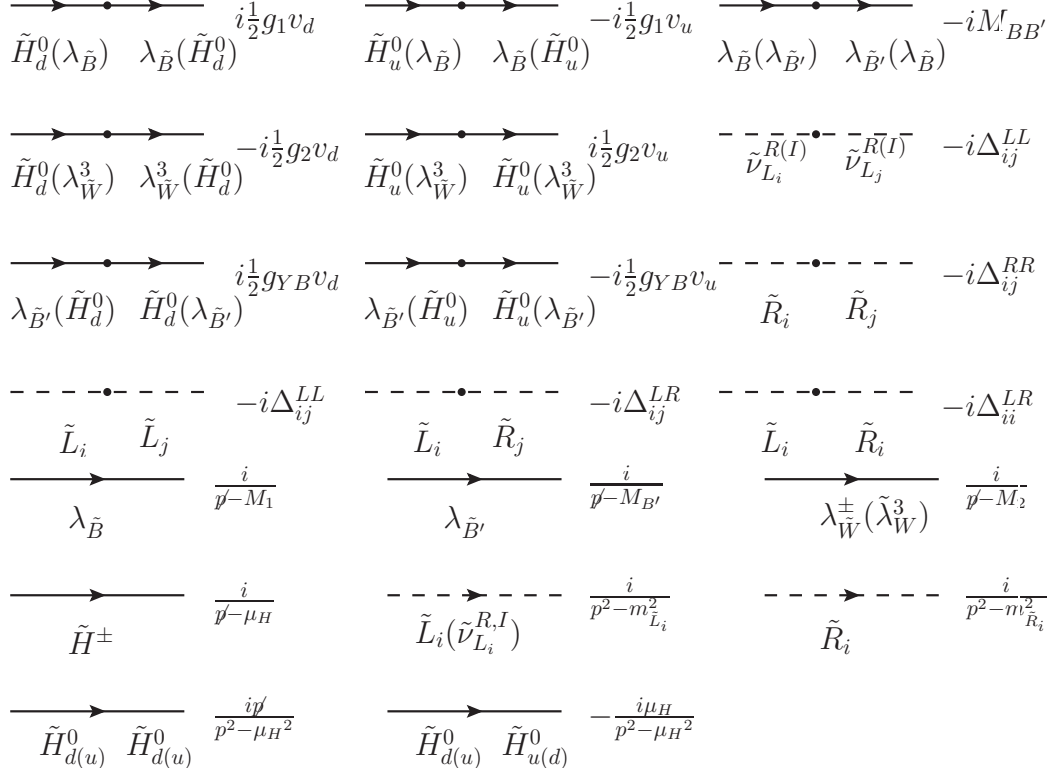


FIG. 13: Feynman rules for the relevant insertions and relevant propagators

$$\begin{aligned}
H_R^{\bar{l}_j \bar{l}_k \tilde{\chi}_i^0} &= [H_L^{l_j \bar{l}_k \tilde{\chi}_i^0}]^*, H_L^{\bar{l}_j \bar{l}_k \tilde{\chi}_i^0} = [H_R^{l_j \bar{l}_k \tilde{\chi}_i^0}]^*, H_R^{\bar{l}_j \tilde{\nu}_k^I \chi_i^\pm} = [H_L^{l_j \tilde{\nu}_k^I \chi_i^\pm}]^*, \\
H_L^{\bar{l}_j \tilde{\nu}_k^I \chi_i^\pm} &= [H_R^{l_j \tilde{\nu}_k^I \chi_i^\pm}]^*, H_R^{\bar{l}_j \tilde{\nu}_k^R \chi_i^\pm} = [H_L^{l_j \tilde{\nu}_k^R \chi_i^\pm}]^*, H_L^{\bar{l}_j \tilde{\nu}_k^R \chi_i^\pm} = [H_R^{l_j \tilde{\nu}_k^R \chi_i^\pm}]^*.
\end{aligned}$$

Appendix C: The relevant Feynman rules in the electroweak interaction basis

The relevant Feynman rules for the present computation are collected in Fig.13.

Appendix D: The contributions from Feynman diagrams with the MIA method

To save space in the text, we use some symbols to represent the coupling vertices associated with the Z boson, as follows:

$$C_L = -g_1 \sin \theta \cos \theta' + g_2 \cos \theta \cos \theta' + (g_{YB} + g_B) \sin \theta', \quad (D1)$$

$$C_R = 2g_1 \sin \theta \cos \theta' - (2g_{YB} + g_B) \sin \theta', \quad (D2)$$

$$E = -\frac{1}{2}(g_2 \cos \theta \cos \theta' - g_1 \sin \theta \cos \theta' + g_{YB} \sin \theta'). \quad (D3)$$

The one-loop contributions from Fig.2(1a)

$$A_R^{S_1}(1a) = \frac{1}{2\Lambda^3} m_{l_i} g_1^2 \Delta_{ij}^{LR} E[G_4(x_{\mu_H}, x_{\tilde{R}_j}, x_{\tilde{L}_i}, x_1)(\sqrt{x_1} - \sqrt{x_{\mu_H}} \tan \beta) - 2\sqrt{x_1} x_{\mu_H} G_5(x_{\mu_H}, \tilde{x}_{R_j}, x_{\tilde{L}_i}, x_1)], \quad (D4)$$

$$A_R^{S_2}(1a) = \frac{1}{4\Lambda^3} m_{l_i} g_{YB} (g_B + 2g_{YB}) \Delta_{ij}^{LR} E[G_4(x_{\mu_H}, x_{\tilde{R}_j}, x_{\tilde{L}_i}, x_{B'}) (\sqrt{x_{B'}} - \sqrt{x_{\mu_H}} \tan \beta) - 2\sqrt{x_{B'}} x_{\mu_H} G_5(x_{\mu_H}, x_{\tilde{R}_j}, x_{\tilde{L}_i}, x_{B'})]. \quad (D5)$$

The one-loop contributions from Fig.2(1b)

$$A_L^{S_1}(1b) = \frac{1}{4\Lambda^3} m_{l_i} g_1^2 \Delta_{ij}^{LR} E[G_4(x_{\mu_H}, x_{\tilde{L}_j}, x_{\tilde{R}_i}, x_1)(\sqrt{x_1} - \sqrt{x_{\mu_H}} \tan \beta) - 2\sqrt{x_1} x_{\mu_H} G_5(x_{\mu_H}, x_{\tilde{L}_j}, x_{\tilde{R}_i}, x_1)], \quad (D6)$$

$$A_L^{S_2}(1b) = \frac{1}{4\Lambda^3} m_{l_i} g_{YB} (g_B + g_{YB}) \Delta_{ij}^{LR} E[G_4(x_{\mu_H}, x_{\tilde{L}_j}, x_{\tilde{R}_i}, x_{B'}) (\sqrt{x_{B'}} - \sqrt{x_{\mu_H}} \tan \beta) - 2\sqrt{x_{B'}} x_{\mu_H} G_5(x_{\mu_H}, x_{\tilde{L}_j}, x_{\tilde{R}_i}, x_{B'})], \quad (D7)$$

$$A_L^{S_3}(1b) = -\frac{1}{4\Lambda^3} m_{l_i} g_2^2 \Delta_{ij}^{LR} E[G_4(x_{\mu_H}, x_{\tilde{L}_j}, x_{R_i}, x_2)(\sqrt{x_2} - \sqrt{x_{\mu_H}} \tan \beta) - 2\sqrt{x_2} x_{\mu_H} G_5(x_{\mu_H}, x_{\tilde{L}_j}, x_{\tilde{R}_i}, x_2)], \quad (D8)$$

The one-loop contributions from Fig.2(1c)

$$A_R^{S_1}(1c) = \frac{1}{2\Lambda^3} m_{l_j} g_1^2 \Delta_{ij}^{LR} E[G_4(x_{\mu_H}, x_{\tilde{L}_j}, x_{\tilde{R}_i}, x_1)(\sqrt{x_1} - \sqrt{x_{\mu_H}} \tan \beta) - 2\sqrt{x_1} x_{\mu_H} G_5(x_{\mu_H}, x_{\tilde{L}_j}, x_{\tilde{R}_i}, x_1)], \quad (D9)$$

$$A_R^{S_2}(1c) = \frac{1}{4\Lambda^3} m_{l_j} g_{YB} (g_B + 2g_{YB}) \Delta_{ij}^{LR} E[G_4(x_{\mu_H}, x_{\tilde{L}_j}, x_{\tilde{R}_i}, x_{B'}) (\sqrt{x_{B'}} - \sqrt{x_{\mu_H}} \tan \beta) - 2\sqrt{x_{B'}} x_{\mu_H} G_5(x_{\mu_H}, x_{\tilde{L}_j}, x_{\tilde{R}_i}, x_{B'})]. \quad (D10)$$

The one-loop contributions from Fig.2(1d)

$$A_L^{S_1}(1d) = \frac{1}{4\Lambda^3} m_{l_j} g_1^2 \Delta_{ij}^{LR} E[G_4(x_{\mu_H}, x_{\tilde{R}_j}, x_{L_i}, x_1)(\sqrt{x_1} - \sqrt{x_{\mu_H}} \tan \beta) - 2\sqrt{x_1} x_{\mu_H} G_5(x_{\mu_H}, x_{\tilde{R}_j}, x_{\tilde{L}_i}, x_1)], \quad (D11)$$

$$A_L^{S_2}(1d) = \frac{1}{4\Lambda^3} m_{l_j} g_{YB} (g_B + g_{YB}) \Delta_{ij}^{LR} E[G_4(x_{\mu_H}, x_{\tilde{R}_j}, x_{\tilde{L}_i}, x_{B'}) (\sqrt{x_{B'}} - \sqrt{x_{\mu_H}} \tan \beta) - 2\sqrt{x_{B'}} x_{\mu_H} G_5(x_{\mu_H}, x_{\tilde{R}_j}, x_{\tilde{L}_i}, x_{B'})], \quad (D12)$$

$$A_L^{S_3}(1d) = -\frac{1}{4\Lambda^3} m_{l_j} g_2^2 \Delta_{ij}^{LR} E[G_4(x_{\mu_H}, x_{\tilde{R}_j}, x_{\tilde{L}_i}, x_2)(\sqrt{x_2} - \sqrt{x_{\mu_H}} \tan \beta) - 2\sqrt{x_2} x_{\mu_H} G_5(x_{\mu_H}, x_{\tilde{R}_j}, x_{\tilde{L}_i}, x_2)]. \quad (D13)$$

The one-loop contributions from Fig.2(1e)

$$A_R^{S_4}(1e) = -\frac{1}{2\Lambda^2} Y_{e,ii} Y_{e,jj} \Delta_{ij}^{LL} E[G_3(x_{\mu_H}, x_{\tilde{L}_j}, x_{\tilde{L}_i}) - 2I_2(x_{\mu_H}, x_{\tilde{L}_j}, x_{\tilde{L}_i})]. \quad (D14)$$

The one-loop contributions from Fig.2(1f)

$$A_L^{S4}(1f) = -\frac{1}{2\Lambda^2} Y_{e,ii} Y_{e,jj} \Delta_{ij}^{RR} E [G_3(x_{\mu_H}, x_{\tilde{R}_j}, x_{\tilde{R}_i}) - 2I_2(x_{\mu_H}, x_{\tilde{R}_j}, x_{\tilde{R}_i})]. \quad (D15)$$

The one-loop contributions from Fig.2(1g)

$$A_R^{S1}(1g) = -\frac{1}{2\Lambda^5} m_{l_i} g_1^2 [G_6(x_{\mu_H}, x_{\tilde{R}_j}, x_{\tilde{R}_i}, x_{\tilde{L}_i}, x_1) (\sqrt{x_1} - \sqrt{x_{\mu_H}} \tan \beta) - 2\sqrt{x_1} x_{\mu_H} G_7(x_{\mu_H}, \tilde{x}_{R_j}, x_{\tilde{R}_i}, x_{\tilde{L}_i}, x_1)] \Delta_{ii}^{LR} \Delta_{ij}^{RR} E, \quad (D16)$$

$$A_R^{S2}(1g) = -\frac{1}{4\Lambda^5} m_{l_i} g_{YB} (g_B + 2g_{YB}) [G_6(x_{\mu_H}, x_{\tilde{R}_j}, x_{\tilde{L}_i}, x_{B'}) (\sqrt{x_{B'}} - \sqrt{x_{\mu_H}} \tan \beta) - 2\sqrt{x_{B'}} x_{\mu_H} G_7(x_{\mu_H}, \tilde{x}_{R_j}, x_{\tilde{R}_i}, x_{\tilde{L}_i}, x_{B'})] \Delta_{ii}^{LR} \Delta_{ij}^{RR} E. \quad (D17)$$

The one-loop contributions from Fig.2(1h)

$$A_L^{S1}(1h) = -\frac{1}{4\Lambda^5} m_{l_i} g_1^2 [G_6(x_{\mu_H}, x_{\tilde{L}_j}, x_{\tilde{L}_i}, x_{\tilde{R}_i}, x_1) (\sqrt{x_1} - \sqrt{x_{\mu_H}} \tan \beta) - 2\sqrt{x_1} x_{\mu_H} G_7(x_{\mu_H}, x_{\tilde{L}_j}, x_{\tilde{L}_i}, x_{\tilde{R}_i}, x_1)] \Delta_{ii}^{LR} \Delta_{ij}^{LL} E, \quad (D18)$$

$$A_L^{S2}(1h) = -\frac{1}{4\Lambda^5} m_{l_i} g_{YB} (g_B + g_{YB}) [G_6(x_{\mu_H}, x_{\tilde{L}_j}, x_{\tilde{L}_i}, x_{\tilde{R}_i}, x_{B'}) (\sqrt{x_{B'}} - \sqrt{x_{\mu_H}} \tan \beta) - 2\sqrt{x_{B'}} x_{\mu_H} G_7(x_{\mu_H}, x_{\tilde{L}_j}, x_{\tilde{L}_i}, x_{\tilde{R}_i}, x_{B'})] \Delta_{ii}^{LR} \Delta_{ij}^{LL} E, \quad (D19)$$

$$A_L^{S3}(1h) = \frac{1}{4\Lambda^5} m_{l_i} g_2^2 [G_6(x_{\mu_H}, x_{\tilde{L}_j}, x_{\tilde{L}_i}, x_{R_i}, x_2) (\sqrt{x_2} - \sqrt{x_{\mu_H}} \tan \beta) - 2\sqrt{x_2} x_{\mu_H} G_7(x_{\mu_H}, x_{\tilde{L}_j}, x_{\tilde{L}_i}, x_{\tilde{R}_i}, x_2)] \Delta_{ii}^{LR} \Delta_{ij}^{LL} E. \quad (D20)$$

The one-loop contributions from Fig.2(1i)

$$A_R^{S1}(1i) = -\frac{1}{2\Lambda^5} m_{l_j} g_1^2 [G_6(x_{\mu_H}, x_{\tilde{L}_j}, x_{\tilde{L}_i}, x_{\tilde{R}_i}, x_1) (\sqrt{x_1} - \sqrt{x_{\mu_H}} \tan \beta) - 2\sqrt{x_1} x_{\mu_H} G_7(x_{\mu_H}, x_{\tilde{L}_j}, x_{\tilde{L}_i}, x_{\tilde{R}_i}, x_1)] \Delta_{ii}^{LR} \Delta_{ij}^{LL} E, \quad (D21)$$

$$A_R^{S2}(1i) = -\frac{1}{4\Lambda^5} m_{l_j} g_{YB} (g_B + 2g_{YB}) [G_6(x_{\mu_H}, x_{\tilde{L}_j}, x_{\tilde{L}_i}, x_{\tilde{R}_i}, x_{B'}) (\sqrt{x_{B'}} - \sqrt{x_{\mu_H}} \tan \beta) - 2\sqrt{x_{B'}} x_{\mu_H} G_7(x_{\mu_H}, x_{\tilde{L}_j}, x_{\tilde{L}_i}, x_{\tilde{R}_i}, x_{B'})] \Delta_{ii}^{LR} \Delta_{ij}^{LL} E. \quad (D22)$$

The one-loop contributions from Fig.2(1j)

$$A_L^{S1}(1j) = -\frac{1}{4\Lambda^5} m_{l_j} g_1^2 [G_6(x_{\mu_H}, x_{\tilde{R}_j}, x_{\tilde{R}_i}, x_{L_i}, x_1) (\sqrt{x_1} - \sqrt{x_{\mu_H}} \tan \beta) - 2\sqrt{x_1} x_{\mu_H} G_7(x_{\mu_H}, x_{\tilde{R}_j}, x_{\tilde{R}_i}, x_{\tilde{L}_i}, x_1)] \Delta_{ii}^{LR} \Delta_{ij}^{RR} E, \quad (D23)$$

$$A_L^{S2}(1j) = -\frac{1}{4\Lambda^5} m_{l_j} g_{YB} (g_B + g_{YB}) [G_6(x_{\mu_H}, x_{\tilde{R}_j}, x_{\tilde{R}_i}, x_{\tilde{L}_i}, x_{B'}) (\sqrt{x_{B'}} - \sqrt{x_{\mu_H}} \tan \beta) - 2\sqrt{x_{B'}} x_{\mu_H} G_7(x_{\mu_H}, x_{\tilde{R}_j}, x_{\tilde{R}_i}, x_{\tilde{L}_i}, x_{B'})] \Delta_{ii}^{LR} \Delta_{ij}^{RR} E, \quad (D24)$$

$$A_L^{S3}(1j) = \frac{1}{4\Lambda^5} m_{l_j} g_2^2 [G_6(x_{\mu_H}, x_{\tilde{R}_j}, x_{\tilde{R}_i}, x_{\tilde{L}_i}, x_2) (\sqrt{x_2} - \sqrt{x_{\mu_H}} \tan \beta) - 2\sqrt{x_2} x_{\mu_H} G_7(x_{\mu_H}, x_{\tilde{R}_j}, x_{\tilde{R}_i}, x_{\tilde{L}_i}, x_2)] \Delta_{ii}^{LR} \Delta_{ij}^{RR} E. \quad (D25)$$

The one-loop contributions from Fig.2(1k)

$$A_R^{S1}(1k) = -\frac{1}{2\Lambda^5} m_{l_i} g_1^2 [G_6(x_{\mu_H}, x_{\tilde{R}_j}, x_{\tilde{L}_j}, x_{\tilde{L}_i}, x_1)(\sqrt{x_1} - \sqrt{x_{\mu_H}} \tan \beta) - 2\sqrt{x_1} x_{\mu_H} G_7(x_{\mu_H}, \tilde{x}_{R_j}, x_{\tilde{L}_j}, x_{\tilde{L}_i}, x_1)] \Delta_{jj}^{LR} \Delta_{ij}^{LL} E, \quad (D26)$$

$$A_R^{S2}(1k) = -\frac{1}{4\Lambda^5} m_{l_i} g_{YB} (g_B + 2g_{YB}) [G_6(x_{\mu_H}, x_{\tilde{R}_j}, x_{\tilde{L}_j}, x_{\tilde{L}_i}, x_{B'}) (\sqrt{x_{B'}} - \sqrt{x_{\mu_H}} \tan \beta) - 2\sqrt{x_{B'}} x_{\mu_H} G_7(x_{\mu_H}, \tilde{x}_{R_j}, x_{\tilde{L}_j}, x_{\tilde{L}_i}, x_{B'})] \Delta_{jj}^{LR} \Delta_{ij}^{LL} E. \quad (D27)$$

The one-loop contributions from Fig.2(1l)

$$A_L^{S1}(1l) = -\frac{1}{4\Lambda^5} m_{l_i} g_1^2 [G_6(x_{\mu_H}, x_{\tilde{L}_j}, x_{\tilde{R}_j}, x_{\tilde{R}_i}, x_1)(\sqrt{x_1} - \sqrt{x_{\mu_H}} \tan \beta) - 2\sqrt{x_1} x_{\mu_H} G_7(x_{\mu_H}, x_{\tilde{L}_j}, x_{\tilde{R}_j}, x_{\tilde{R}_i}, x_1)] \Delta_{jj}^{LR} \Delta_{ij}^{RR} E, \quad (D28)$$

$$A_L^{S2}(1l) = -\frac{1}{4\Lambda^5} m_{l_i} g_{YB} (g_B + g_{YB}) [G_6(x_{\mu_H}, x_{\tilde{L}_j}, x_{\tilde{R}_j}, x_{\tilde{R}_i}, x_{B'}) (\sqrt{x_{B'}} - \sqrt{x_{\mu_H}} \tan \beta) - 2\sqrt{x_{B'}} x_{\mu_H} G_7(x_{\mu_H}, x_{\tilde{L}_j}, x_{\tilde{R}_j}, x_{\tilde{R}_i}, x_{B'})] \Delta_{jj}^{LR} \Delta_{ij}^{RR} E, \quad (D29)$$

$$A_L^{S3}(1l) = \frac{1}{4\Lambda^5} m_{l_i} g_2^2 [G_6(x_{\mu_H}, x_{\tilde{L}_j}, x_{\tilde{R}_j}, x_{R_i}, x_2)(\sqrt{x_2} - \sqrt{x_{\mu_H}} \tan \beta) - 2\sqrt{x_2} x_{\mu_H} G_7(x_{\mu_H}, x_{\tilde{L}_j}, x_{\tilde{R}_j}, x_{R_i}, x_2)] \Delta_{jj}^{LR} \Delta_{ij}^{RR} E. \quad (D30)$$

The one-loop contributions from Fig.2(1m)

$$A_R^{S1}(1m) = -\frac{1}{2\Lambda^5} m_{l_j} g_1^2 [G_6(x_{\mu_H}, x_{\tilde{L}_j}, x_{\tilde{R}_j}, x_{\tilde{R}_i}, x_1)(\sqrt{x_1} - \sqrt{x_{\mu_H}} \tan \beta) - 2\sqrt{x_1} x_{\mu_H} G_7(x_{\mu_H}, x_{\tilde{L}_j}, x_{\tilde{R}_j}, x_{\tilde{R}_i}, x_1)] \Delta_{jj}^{LR} \Delta_{ij}^{RR} E, \quad (D31)$$

$$A_R^{S2}(1m) = -\frac{1}{4\Lambda^5} m_{l_j} g_{YB} (g_B + 2g_{YB}) [G_6(x_{\mu_H}, x_{\tilde{L}_j}, x_{\tilde{R}_j}, x_{\tilde{R}_i}, x_{B'}) (\sqrt{x_{B'}} - \sqrt{x_{\mu_H}} \tan \beta) - 2\sqrt{x_{B'}} x_{\mu_H} G_7(x_{\mu_H}, x_{\tilde{L}_j}, x_{\tilde{R}_j}, x_{\tilde{R}_i}, x_{B'})] \Delta_{jj}^{LR} \Delta_{ij}^{RR} E. \quad (D32)$$

The one-loop contributions from Fig.2(1n)

$$A_L^{S1}(1n) = -\frac{1}{4\Lambda^5} m_{l_j} g_1^2 [G_6(x_{\mu_H}, x_{\tilde{R}_j}, x_{\tilde{L}_j}, x_{L_i}, x_1)(\sqrt{x_1} - \sqrt{x_{\mu_H}} \tan \beta) - 2\sqrt{x_1} x_{\mu_H} G_7(x_{\mu_H}, x_{\tilde{R}_j}, x_{\tilde{L}_j}, x_{L_i}, x_1)] \Delta_{jj}^{LR} \Delta_{ij}^{LL} E, \quad (D33)$$

$$A_L^{S2}(1n) = -\frac{1}{4\Lambda^5} m_{l_j} g_{YB} (g_B + g_{YB}) [G_6(x_{\mu_H}, x_{\tilde{R}_j}, x_{\tilde{L}_j}, x_{L_i}, x_{B'}) (\sqrt{x_{B'}} - \sqrt{x_{\mu_H}} \tan \beta) - 2\sqrt{x_{B'}} x_{\mu_H} G_7(x_{\mu_H}, x_{\tilde{R}_j}, x_{\tilde{L}_j}, x_{L_i}, x_{B'})] \Delta_{jj}^{LR} \Delta_{ij}^{LL} E, \quad (D34)$$

$$A_L^{S3}(1n) = \frac{1}{4\Lambda^5} m_{l_j} g_2^2 [G_6(x_{\mu_H}, x_{\tilde{R}_j}, x_{\tilde{L}_j}, x_{L_i}, x_2)(\sqrt{x_2} - \sqrt{x_{\mu_H}} \tan \beta) - 2\sqrt{x_2} x_{\mu_H} G_7(x_{\mu_H}, x_{\tilde{R}_j}, x_{\tilde{L}_j}, x_{L_i}, x_2)] \Delta_{jj}^{LR} \Delta_{ij}^{LL} E. \quad (D35)$$

The one-loop contributions from Fig.3(3a)

$$A_R^{S_1}(3a) = \frac{1}{2\Lambda^2} g_1^2 \Delta_{ij}^{RR} C_R [G_3(x_{\tilde{R}_j}, x_1, x_{\tilde{R}_i}) + G_3(x_{\tilde{R}_i}, x_1, x_{\tilde{R}_j})], \quad (D36)$$

$$A_R^{S_2}(3a) = \frac{1}{8\Lambda^2} (g_B + 2g_{YB})^2 \Delta_{ij}^{RR} C_R [G_3(x_{\tilde{R}_j}, x_{B'}, x_{\tilde{R}_i}) + G_3(x_{\tilde{R}_i}, x_{B'}, x_{\tilde{R}_j})], \quad (D37)$$

$$A_L^{S_4}(3a) = \frac{1}{4\Lambda^2} Y_{e,ii} Y_{e,jj} C_R \Delta_{ij}^{RR} [G_3(x_{\tilde{R}_j}, x_{\mu_H}, x_{\tilde{R}_i}) + G_3(x_{\tilde{R}_i}, x_{\mu_H}, x_{\tilde{R}_j})]. \quad (D38)$$

The one-loop contributions from Fig.3(3b)

$$A_L^{S_1}(3b) = -\frac{1}{8\Lambda^2} g_1^2 \Delta_{ij}^{LL} C_L [G_3(x_{\tilde{L}_j}, x_1, x_{\tilde{L}_i}) + G_3(x_{\tilde{L}_i}, x_1, x_{\tilde{L}_j})], \quad (D39)$$

$$A_L^{S_2}(3b) = -\frac{1}{8\Lambda^2} (g_B + g_{YB})^2 \Delta_{ij}^{LL} C_L [G_3(x_{\tilde{L}_j}, x_{B'}, x_{\tilde{L}_i}) + G_3(x_{\tilde{L}_i}, x_{B'}, x_{\tilde{L}_j})], \quad (D40)$$

$$A_L^{S_3}(3b) = -\frac{1}{8\Lambda^2} g_2^2 C_L \Delta_{ij}^{LL} [G_3(x_{\tilde{L}_j}, x_2, x_{\tilde{L}_i}) + G_3(x_{\tilde{L}_i}, x_2, x_{\tilde{L}_j})], \quad (D41)$$

$$A_R^{S_4}(3b) = -\frac{1}{4\Lambda^2} Y_{e,ii} Y_{e,jj} C_L \Delta_{ij}^{LL} [G_3(x_{\tilde{L}_j}, x_{\mu_H}, x_{\tilde{L}_i}) + G_3(x_{\tilde{L}_i}, x_{\mu_H}, x_{\tilde{L}_j})]. \quad (D42)$$

The one-loop contributions from Fig.3(3c)

$$A_L^{S_{1(2)}-S_{2(1)}}(3c) = \frac{1}{4\Lambda^2} (\sqrt{x_1} + \sqrt{x_{B'}}) g_1 (g_B + 2g_{YB}) \Delta_{ij}^{RR} \sqrt{x_{BB'}} C_R \\ \times [G_4(x_{\tilde{R}_j}, x_1, x_{\tilde{R}_i}, x_{B'}) + G_4(x_{\tilde{R}_i}, x_1, x_{\tilde{R}_j}, x_{B'})]. \quad (D43)$$

The one-loop contributions from Fig.3(3d)

$$A_L^{S_{1(2)}-S_{2(1)}}(3d) = -\frac{1}{8\Lambda^2} (\sqrt{x_1} + \sqrt{x_{B'}}) g_1 (g_B + g_{YB}) \Delta_{ij}^{LL} \sqrt{x_{BB'}} C_L \\ \times [G_4(x_{\tilde{L}_j}, x_1, x_{\tilde{L}_i}, x_{B'}) + G_4(x_{\tilde{L}_i}, x_1, x_{\tilde{L}_j}, x_{B'})]. \quad (D44)$$

The one-loop contributions from Fig.3(3e)

$$A_R^{S_1}(3e) = \frac{1}{4\Lambda^3} (\sqrt{x_{\mu_H}} \tan \beta + \sqrt{x_1}) m_{l_j} g_1^2 \Delta_{ij}^{LR} \\ \times [C_L G_4(x_{\tilde{L}_j}, x_{\mu_H}, x_{\tilde{R}_i}, x_1) - C_R G_4(x_{\tilde{R}_i}, x_{\mu_H}, x_{\tilde{L}_j}, x_1)], \quad (D45)$$

$$A_R^{S_2}(3e) = \frac{1}{8\Lambda^3} (\sqrt{x_{\mu_H}} \tan \beta + \sqrt{x_{B'}}) m_{l_j} g_{YB} (g_B + 2g_{YB}) \Delta_{ij}^{LR} \\ \times [C_L G_4(x_{\tilde{L}_j}, x_{\mu_H}, x_{\tilde{R}_i}, x_{B'}) - C_R G_4(x_{\tilde{R}_i}, x_{\mu_H}, x_{\tilde{L}_j}, x_{B'})]. \quad (D46)$$

The one-loop contributions from Fig.3(3f)

$$A_L^{S_1}(3f) = \frac{1}{8\Lambda^3}(\sqrt{x_{\mu_H}} \tan \beta + \sqrt{x_1})m_{l_j}g_1^2\Delta_{ij}^{LR} \\ \times [C_R G_4(x_{\tilde{R}_j}, x_{\mu_H}, x_{\tilde{L}_i}, x_1) - C_L G_4(x_{\tilde{L}_i}, x_{\mu_H}, x_{\tilde{R}_j}, x_1)], \quad (D47)$$

$$A_L^{S_2}(3f) = \frac{1}{8\Lambda^3}(\sqrt{x_{\mu_H}} \tan \beta + \sqrt{x_{B'}})m_{l_j}g_{YB}(g_B + 2g_{YB})\Delta_{ij}^{LR} \\ \times [C_R G_4(x_{\tilde{R}_j}, x_{\mu_H}, x_{\tilde{L}_i}, x_{B'}) - C_L G_4(x_{\tilde{L}_i}, x_{\mu_H}, x_{\tilde{R}_j}, x_{B'})], \quad (D48)$$

$$A_L^{S_3}(3f) = -\frac{1}{8\Lambda^3}(\sqrt{x_{\mu_H}} \tan \beta + \sqrt{x_2})m_{l_j}g_2^2\Delta_{ij}^{LR} \\ \times [C_R G_4(x_{\tilde{R}_j}, x_{\mu_H}, x_{\tilde{L}_i}, x_2) - C_L G_4(x_{\tilde{L}_i}, x_{\mu_H}, x_{\tilde{R}_j}, x_2)]. \quad (D49)$$

The one-loop contributions from Fig.3(3g)

$$A_R^{S_1}(3g) = -\frac{1}{4\Lambda^3}m_{l_i}g_1^2(\sqrt{x_1} + \sqrt{x_{\mu_H}} \tan \beta)\Delta_{ij}^{LR} \\ \times [C_R G_4(x_{\tilde{R}_j}, x_{\mu_H}, x_{\tilde{L}_i}, x_1) - C_L G_4(x_{\tilde{L}_i}, x_{\mu_H}, x_{\tilde{R}_j}, x_1)], \quad (D50)$$

$$A_R^{S_2}(3g) = -\frac{1}{8\Lambda^3}m_{l_i}g_{YB}(g_B + 2g_{YB})(\sqrt{x_{B'}} + \sqrt{x_{\mu_H}} \tan \beta)\Delta_{ij}^{LR} \\ \times [C_R G_4(x_{\tilde{R}_j}, x_{\mu_H}, x_{\tilde{L}_i}, x_{B'}) - C_L G_4(x_{\tilde{L}_i}, x_{\mu_H}, x_{\tilde{R}_j}, x_{B'})]. \quad (D51)$$

The one-loop contributions from Fig.3(3h)

$$A_L^{S_1}(3h) = -\frac{1}{8\Lambda^3}m_{l_i}g_1^2(\sqrt{x_1} + \sqrt{x_{\mu_H}} \tan \beta)\Delta_{ij}^{LR} \\ \times [C_L G_4(x_{\tilde{L}_j}, x_{\mu_H}, x_{\tilde{R}_i}, x_1) - C_R G_4(x_{\tilde{R}_i}, x_{\mu_H}, x_{\tilde{L}_j}, x_1)], \quad (D52)$$

$$A_L^{S_2}(3h) = -\frac{1}{8\Lambda^3}m_{l_i}g_{YB}(g_B + g_{YB})(\sqrt{x_{B'}} + \sqrt{x_{\mu_H}} \tan \beta)\Delta_{ij}^{LR} \\ \times [C_L G_4(x_{\tilde{L}_j}, x_{\mu_H}, x_{\tilde{R}_i}, x_{B'}) - C_R G_4(x_{\tilde{R}_i}, x_{\mu_H}, x_{\tilde{L}_j}, x_{B'})], \quad (D53)$$

$$A_L^{S_3}(3h) = \frac{1}{8\Lambda^3}(\sqrt{x_{\mu_H}} \tan \beta + \sqrt{x_2})m_{l_i}g_2^2\Delta_{ij}^{LR} \\ \times [C_L G_4(x_{\tilde{L}_j}, x_{\mu_H}, x_{\tilde{R}_i}, x_2) - C_R G_4(x_{\tilde{R}_i}, x_{\mu_H}, x_{\tilde{L}_j}, x_2)]. \quad (D54)$$

The one-loop contributions from Fig.3(3i)

$$\begin{aligned}
A_L^{S_1}(3i) &= -\frac{1}{8\Lambda^5}(\sqrt{x_{\mu_H}} \tan \beta + \sqrt{x_1})m_{l_j}g_1^2\Delta_{jj}^{LR}\Delta_{ij}^{LL} \\
&\quad \times [C_R G_6(x_{\tilde{R}_j}, x_{\mu_H}, x_{\tilde{L}_i}, x_{\tilde{L}_j}, x_1) \\
&\quad - C_L(G_6(x_{\tilde{L}_i}, x_{\mu_H}, x_{\tilde{R}_j}, x_1) + G_6(x_{\tilde{L}_j}x_{\tilde{L}_i}, x_{\mu_H}, x_{\tilde{R}_j}, x_1))], \tag{D55}
\end{aligned}$$

$$\begin{aligned}
A_L^{S_2}(3i) &= -\frac{1}{8\Lambda^5}(\sqrt{x_{\mu_H}} \tan \beta + \sqrt{x_{B'}})m_{l_j}g_{YB}(g_B + g_{YB})\Delta_{jj}^{LR}\Delta_{ij}^{LL} \\
&\quad \times [C_R G_6(x_{\tilde{R}_j}, x_{\mu_H}, x_{\tilde{L}_i}, x_{\tilde{L}_j}x_{B'}) \\
&\quad - C_L(G_6(x_{\tilde{L}_i}, x_{\mu_H}, x_{\tilde{R}_j}, x_{B'}) + G_6(x_{\tilde{L}_j}x_{\tilde{L}_i}, x_{\mu_H}, x_{\tilde{R}_j}, x_{B'}))], \tag{D56}
\end{aligned}$$

$$\begin{aligned}
A_L^{S_3}(3i) &= \frac{1}{8\Lambda^5}(\sqrt{x_{\mu_H}} \tan \beta + \sqrt{x_2})m_{l_j}g_2^2\Delta_{jj}^{LR}\Delta_{ij}^{LL} \\
&\quad \times [C_R G_6(x_{\tilde{R}_j}, x_{\mu_H}, x_{\tilde{L}_i}, x_{\tilde{L}_j}, x_2) \\
&\quad - C_L(G_6(x_{\tilde{L}_i}, x_{\mu_H}, x_{\tilde{R}_j}, x_2) + G_6(x_{\tilde{L}_j}x_{\tilde{L}_i}, x_{\mu_H}, x_{\tilde{R}_j}, x_2))]. \tag{D57}
\end{aligned}$$

The one-loop contributions from Fig.3(3j)

$$\begin{aligned}
A_R^{S_1}(3j) &= -\frac{1}{4\Lambda^5}(\sqrt{x_{\mu_H}} \tan \beta + \sqrt{x_1})m_{l_j}g_1^2\Delta_{ii}^{LR}\Delta_{ij}^{LL} \\
&\quad \times [C_L(G_6(x_{\tilde{L}_j}, x_{\tilde{L}_i}, x_{\mu_H}, x_{\tilde{R}_i}, x_1) + G_6(x_{\tilde{L}_i}, x_{\tilde{L}_j}, x_{\mu_H}, x_{\tilde{R}_i}, x_1)) \\
&\quad - C_R G_6(x_{\tilde{R}_i}, x_{\mu_H}, x_{\tilde{L}_j}, x_{\tilde{L}_i}, x_1)], \tag{D58}
\end{aligned}$$

$$\begin{aligned}
A_R^{S_2}(3j) &= -\frac{1}{8\Lambda^5}(\sqrt{x_{\mu_H}} \tan \beta + \sqrt{x_{B'}})m_{l_j}g_{YB}(g_B + 2g_{YB})\Delta_{ii}^{LR}\Delta_{ij}^{LL} \\
&\quad \times [C_L(G_6(x_{\tilde{L}_j}, x_{\tilde{L}_i}, x_{\mu_H}, x_{\tilde{R}_i}, x_{B'}) + G_6(x_{\tilde{L}_i}, x_{\tilde{L}_j}, x_{\mu_H}, x_{\tilde{R}_i}x_{B'})) \\
&\quad - C_R G_6(x_{\tilde{R}_i}, x_{\mu_H}, x_{\tilde{L}_j}, x_{\tilde{L}_i}x_{B'})]. \tag{D59}
\end{aligned}$$

The one-loop contributions from Fig.3(3k)

$$\begin{aligned}
A_R^{S_1}(3k) &= \frac{1}{4\Lambda^5}m_{l_i}g_1^2(\sqrt{x_1} + \sqrt{x_{\mu_H}} \tan \beta)\Delta_{jj}^{LR}\Delta_{ij}^{LL} \\
&\quad \times [C_R G_6(x_{\tilde{R}_j}, x_{\mu_H}, x_{\tilde{L}_i}, x_{\tilde{L}_j}, x_1) \\
&\quad - C_L(G_6(x_{\tilde{L}_i}, x_{\mu_H}, x_{\tilde{R}_j}, x_1) + G_6(x_{\tilde{L}_j}x_{\tilde{L}_i}, x_{\mu_H}, x_{\tilde{R}_j}, x_1))], \tag{D60}
\end{aligned}$$

$$\begin{aligned}
A_R^{S_2}(3k) &= \frac{1}{8\Lambda^5}m_{l_i}g_{YB}(g_B + 2g_{YB})(\sqrt{x_{B'}} + \sqrt{x_{\mu_H}} \tan \beta)\Delta_{jj}^{LR}\Delta_{ij}^{LL} \\
&\quad \times [C_R G_6(x_{\tilde{R}_j}, x_{\mu_H}, x_{\tilde{L}_j}, x_{\tilde{L}_i}, x_{B'}) \\
&\quad - C_L(G_6(x_{\tilde{L}_i}, x_{\tilde{L}_j}, x_{\mu_H}, x_{\tilde{R}_j}, x_{B'}) + G_6(x_{\tilde{L}_j}, x_{\tilde{L}_i}, x_{\mu_H}, x_{\tilde{R}_j}, x_{B'}))]. \tag{D61}
\end{aligned}$$

The one-loop contributions from Fig.3(3l)

$$\begin{aligned}
A_L^{S_1}(3l) &= \frac{1}{8\Lambda^5} m_{l_i} g_1^2 (\sqrt{x_1} + \sqrt{x_{\mu_H}} \tan \beta) \Delta_{ii}^{LR} \Delta_{ij}^{LL} \\
&\times [C_L(G_6(x_{\tilde{L}_j}, x_{\tilde{L}_i}, x_{\mu_H}, x_{\tilde{R}_i}, x_1) + G_6(x_{\tilde{L}_i}, x_{\tilde{L}_j}, x_{\mu_H}, x_{\tilde{R}_i}, x_1)) \\
&- C_R G_6(x_{\tilde{R}_i}, x_{\mu_H}, x_{\tilde{L}_j}, x_{\tilde{L}_j}, x_1)], \tag{D62}
\end{aligned}$$

$$\begin{aligned}
A_L^{S_2}(3l) &= \frac{1}{8\Lambda^5} m_{l_i} g_{YB} (g_B + g_{YB}) (\sqrt{x_{B'}} + \sqrt{x_{\mu_H}} \tan \beta) \Delta_{ii}^{LR} \Delta_{ij}^{LL} \\
&\times [C_L(G_6(x_{\tilde{L}_j}, x_{\tilde{L}_i}, x_{\mu_H}, x_{\tilde{R}_i}, x_{B'}) + G_6(x_{\tilde{L}_i}, x_{\tilde{L}_j}, x_{\mu_H}, x_{\tilde{R}_i}, x_{B'})) \\
&- C_R G_6(x_{\tilde{R}_i}, x_{\mu_H}, x_{\tilde{L}_j}, x_{\tilde{L}_j}, x_{B'})], \tag{D63}
\end{aligned}$$

$$\begin{aligned}
A_L^{S_3}(3l) &= -\frac{1}{8\Lambda^5} (\sqrt{x_{\mu_H}} \tan \beta + \sqrt{x_2}) m_{l_i} g_2^2 \Delta_{ii}^{LR} \Delta_{ij}^{LL} \\
&\times [C_L(G_6(x_{\tilde{L}_j}, x_{\tilde{L}_i}, x_{\mu_H}, x_{\tilde{R}_i}, x_2) + G_6(x_{\tilde{L}_i}, x_{\tilde{L}_j}, x_{\mu_H}, x_{\tilde{R}_i}, x_2)) \\
&- C_R G_6(x_{\tilde{R}_i}, x_{\mu_H}, x_{\tilde{L}_j}, x_{\tilde{L}_j}, x_2)]. \tag{D64}
\end{aligned}$$

The one-loop contributions from Fig.3(3m)

$$\begin{aligned}
A_R^{S_1}(3m) &= -\frac{1}{4\Lambda^5} (\sqrt{x_{\mu_H}} \tan \beta + \sqrt{x_1}) m_{l_j} g_1^2 \Delta_{jj}^{LR} \Delta_{ij}^{RR} \\
&\times [C_L G_6(x_{\tilde{L}_j}, x_{\tilde{R}_j}, x_{\mu_H}, x_{\tilde{R}_i}, x_1) \\
&- C_R (G_6(x_{\tilde{R}_j}, x_{\mu_H}, x_{\tilde{R}_i}, x_{\tilde{L}_j}, x_1) + G_6(x_{\tilde{R}_i}, x_{\mu_H}, x_{\tilde{R}_j}, x_{\tilde{L}_j}, x_1))], \tag{D65}
\end{aligned}$$

$$\begin{aligned}
A_R^{S_2}(3m) &= -\frac{1}{8\Lambda^5} (\sqrt{x_{\mu_H}} \tan \beta + \sqrt{x_{B'}}) m_{l_j} g_{YB} (g_B + 2g_{YB}) \Delta_{jj}^{LR} \Delta_{ij}^{RR} \\
&\times [C_L G_6(x_{\tilde{L}_j}, x_{\tilde{R}_j}, x_{\mu_H}, x_{\tilde{R}_i}, x_{B'}) \\
&- C_R (G_6(x_{\tilde{R}_j}, x_{\mu_H}, x_{\tilde{R}_i}, x_{\tilde{L}_j}, x_{B'}) + G_6(x_{\tilde{R}_i}, x_{\mu_H}, x_{\tilde{R}_j}, x_{\tilde{L}_j}, x_{B'}))]. \tag{D66}
\end{aligned}$$

The one-loop contributions from Fig.3(3n)

$$\begin{aligned}
A_L^{S_1}(3n) &= -\frac{1}{8\Lambda^5} (\sqrt{x_{\mu_H}} \tan \beta + \sqrt{x_1}) m_{l_j} g_1^2 \Delta_{ii}^{LR} \Delta_{ij}^{RR} \\
&\times [C_R (G_6(x_{\tilde{R}_i}, x_{\mu_H}, x_{\tilde{L}_i}, x_{\tilde{R}_j}, x_1) + G_6(x_{\tilde{R}_j}, x_{\mu_H}, x_{\tilde{L}_i}, x_{\tilde{R}_i}, x_1)) \\
&- C_L G_6(x_{\tilde{L}_i}, x_{\tilde{R}_i}, x_{\mu_H}, x_{\tilde{R}_j}, x_1)], \tag{D67}
\end{aligned}$$

$$\begin{aligned}
A_L^{S_2}(3n) &= -\frac{1}{8\Lambda^5} (\sqrt{x_{\mu_H}} \tan \beta + \sqrt{x_{B'}}) m_{l_j} g_{YB} (g_B + g_{YB}) \Delta_{ii}^{LR} \Delta_{ij}^{RR} \\
&\times [C_R (G_6(x_{\tilde{R}_i}, x_{\mu_H}, x_{\tilde{L}_i}, x_{\tilde{R}_j}, x_{B'}) + G_6(x_{\tilde{R}_j}, x_{\mu_H}, x_{\tilde{L}_i}, x_{\tilde{R}_i}, x_{B'})) \\
&- C_L G_6(x_{\tilde{L}_i}, x_{\tilde{R}_i}, x_{\mu_H}, x_{\tilde{R}_j}, x_{B'})], \tag{D68}
\end{aligned}$$

$$\begin{aligned}
A_L^{S_3}(3n) &= \frac{1}{8\Lambda^5} (\sqrt{x_{\mu_H}} \tan \beta + \sqrt{x_2}) m_{l_j} g_2^2 \Delta_{ii}^{LR} \Delta_{ij}^{RR} \\
&\times [C_R (G_6(x_{\tilde{R}_i}, x_{\mu_H}, x_{\tilde{L}_i}, x_{\tilde{R}_j}, x_2) + G_6(x_{\tilde{R}_j}, x_{\mu_H}, x_{\tilde{L}_i}, x_{\tilde{R}_i}, x_2)) \\
&- C_L G_6(x_{\tilde{L}_i}, x_{\tilde{R}_i}, x_{\mu_H}, x_{\tilde{R}_j}, x_2)]. \tag{D69}
\end{aligned}$$

The one-loop contributions from Fig.3(3o)

$$\begin{aligned}
A_R^{S_1}(3o) &= \frac{1}{4\Lambda^5} m_l g_1^2 (\sqrt{x_1} + \sqrt{x_{\mu_H}} \tan \beta) \Delta_{ii}^{LR} \Delta_{ij}^{RR} \\
&\times [C_R(G_6(x_{\tilde{R}_i}, x_{\mu_H}, x_{\tilde{L}_i}, x_{\tilde{R}_j}, x_1) + G_6(x_{\tilde{R}_j}, x_{\mu_H}, x_{\tilde{L}_i}, x_{\tilde{R}_i}, x_1)) \\
&- C_L G_6(x_{\tilde{L}_i}, x_{\tilde{R}_i}, x_{\mu_H}, x_{\tilde{R}_j}, x_1)], \tag{D70}
\end{aligned}$$

$$\begin{aligned}
A_R^{S_2}(3o) &= \frac{1}{8\Lambda^5} m_l g_{YB} (g_B + 2g_{YB}) (\sqrt{x_{B'}} + \sqrt{x_{\mu_H}} \tan \beta) \Delta_{ii}^{LR} \Delta_{ij}^{RR} \\
&\times [C_R(G_6(x_{\tilde{R}_i}, x_{\mu_H}, x_{\tilde{L}_i}, x_{\tilde{R}_j}, x_{B'}) + G_6(x_{\tilde{R}_j}, x_{\mu_H}, x_{\tilde{L}_i}, x_{\tilde{R}_i}, x_{B'})) \\
&- C_L G_6(x_{\tilde{L}_i}, x_{\tilde{R}_i}, x_{\mu_H}, x_{\tilde{R}_j}, x_{B'})]. \tag{D71}
\end{aligned}$$

The one-loop contributions from Fig.3(3p)

$$\begin{aligned}
A_L^{S_1}(3p) &= \frac{1}{8\Lambda^5} m_l g_1^2 (\sqrt{x_1} + \sqrt{x_{\mu_H}} \tan \beta) \Delta_{jj}^{LR} \Delta_{ij}^{RR} \\
&\times [C_L G_6(x_{\tilde{L}_j}, x_{\tilde{R}_j}, x_{\mu_H}, x_{\tilde{R}_i}, x_1) \\
&- C_R(G_6(x_{\tilde{R}_j}, x_{\mu_H}, x_{\tilde{R}_i}, x_{\tilde{L}_j}, x_1) + G_6(x_{\tilde{R}_i}, x_{\mu_H}, x_{\tilde{R}_j}, x_{\tilde{L}_j}, x_1))], \tag{D72}
\end{aligned}$$

$$\begin{aligned}
A_L^{S_2}(3p) &= \frac{1}{8\Lambda^5} m_l g_{YB} (g_B + g_{YB}) (\sqrt{x_{B'}} + \sqrt{x_{\mu_H}} \tan \beta) \Delta_{jj}^{LR} \Delta_{ij}^{RR} \\
&\times [C_L G_6(x_{\tilde{L}_j}, x_{\tilde{R}_j}, x_{\mu_H}, x_{\tilde{R}_i}, x_{B'}) \\
&- C_R(G_6(x_{\tilde{R}_j}, x_{\mu_H}, x_{\tilde{R}_i}, x_{\tilde{L}_j}, x_{B'}) + G_6(x_{\tilde{R}_i}, x_{\mu_H}, x_{\tilde{R}_j}, x_{\tilde{L}_j}, x_{B'}))], \tag{D73}
\end{aligned}$$

$$\begin{aligned}
A_L^{S_3}(3p) &= -\frac{1}{8\Lambda^5} (\sqrt{x_{\mu_H}} \tan \beta + \sqrt{x_2}) m_l g_2^2 \Delta_{jj}^{LR} \Delta_{ij}^{RR} \\
&\times [C_L G_6(x_{\tilde{L}_j}, x_{\tilde{R}_j}, x_{\mu_H}, x_{\tilde{R}_i}, x_2) \\
&- C_R(G_6(x_{\tilde{R}_j}, x_{\mu_H}, x_{\tilde{R}_i}, x_{\tilde{L}_j}, x_2) + G_6(x_{\tilde{R}_i}, x_{\mu_H}, x_{\tilde{R}_j}, x_{\tilde{L}_j}, x_2))]. \tag{D74}
\end{aligned}$$

- [1] L. Calibbi and G. Signorelli, Riv. Nuovo Cim. **41** (2018) no.2, 71-174 doi:10.1393/ncr/i2018-10144-0 [arXiv:1709.00294 [hep-ph]].
- [2] N. Cabibbo, Phys. Rev. Lett. **10** (1963), 531-533 doi:10.1103/PhysRevLett.10.531.
- [3] M. Kobayashi and T. Maskawa, Prog. Theor. Phys. **49** (1973), 652-657 doi:10.1143/PTP.49.652.
- [4] Y. Abe *et al.* [Double Chooz], Phys. Rev. Lett. **108** (2012), 131801 doi:10.1103/PhysRevLett.108.131801 [arXiv:1112.6353 [hep-ex]].
- [5] F. P. An *et al.* [Daya Bay], Phys. Rev. Lett. **108** (2012), 171803 doi:10.1103/PhysRevLett.108.171803 [arXiv:1203.1669 [hep-ex]].

- [6] K. S. Sun, J. B. Chen, X. Y. Yang and S. K. Cui, *Chin. Phys. C* **43** (2019) no.4, 043101 doi:10.1088/1674-1137/43/4/043101 [arXiv:1901.03800 [hep-ph]].
- [7] B. O'Leary, W. Porod and F. Staub, *JHEP* **05** (2012), 042 doi:10.1007/JHEP05(2012)042 [arXiv:1112.4600 [hep-ph]].
- [8] W. Abdallah, S. Khalil and S. Moretti, *Phys. Rev. D* **91** (2015) no.1, 014001 doi:10.1103/PhysRevD.91.014001 [arXiv:1409.7837 [hep-ph]].
- [9] V. Barger, P. Fileviez Perez and S. Spinner, *Phys. Rev. Lett.* **102** (2009), 181802 doi:10.1103/PhysRevLett.102.181802 [arXiv:0812.3661 [hep-ph]].
- [10] P. Fileviez Perez and S. Spinner, *Phys. Lett. B* **673** (2009), 251-254 doi:10.1016/j.physletb.2009.02.047 [arXiv:0811.3424 [hep-ph]].
- [11] P. Fileviez Perez and S. Spinner, *Phys. Rev. D* **83** (2011), 035004 doi:10.1103/PhysRevD.83.035004 [arXiv:1005.4930 [hep-ph]].
- [12] H. P. Nilles, *Phys. Rept.* **110** (1984), 1-162 doi:10.1016/0370-1573(84)90008-5.
- [13] H. E. Haber and G. L. Kane, *Phys. Rept.* **117** (1985), 75-263 doi:10.1016/0370-1573(85)90051-1.
- [14] J. Rosiek, *Phys. Rev. D* **41** (1990), 3464 doi:10.1103/PhysRevD.41.3464.
- [15] C. S. Aulakh, A. Melfo, A. Rasin and G. Senjanovic, *Phys. Lett. B* **459** (1999), 557-562 doi:10.1016/S0370-2693(99)00708-X [arXiv:hep-ph/9902409 [hep-ph]].
- [16] J. M. Yang, *Sci. China Phys. Mech. Astron.* **53** (2010), 1949-1952 doi:10.1007/s11433-010-4146-3 [arXiv:1006.2594 [hep-ph]].
- [17] X. Han, *Mod. Phys. Lett. A* **27** (2012), 1250158 doi:10.1142/S0217732312501581 [arXiv:1104.3534 [hep-ph]].
- [18] H. B. Zhang, T. F. Feng, S. M. Zhao and F. Sun, *Int. J. Mod. Phys. A* **29** (2014), 1450123 doi:10.1142/S0217751X14501231 [arXiv:1407.7365 [hep-ph]].
- [19] X. X. Dong, S. M. Zhao, X. J. Zhan, Z. J. Yang, H. B. Zhang and T. F. Feng, *Chin. Phys. C* **41** (2017) no.7, 073103 doi:10.1088/1674-1137/41/7/073103 [arXiv:1704.02202 [hep-ph]].
- [20] Y. T. Wang, S. M. Zhao, T. T. Wang, X. Wang, X. X. Long, J. Ma and T. F. Feng, *Phys. Rev. D* **106** (2022) no.5, 055044 doi:10.1103/PhysRevD.106.055044 [arXiv:2207.01770 [hep-ph]].
- [21] E. Arganda, M. J. Herrero, R. Morales and A. Szyrkman, *JHEP* **03** (2016), 055 doi:10.1007/JHEP03(2016)055 [arXiv:1510.04685 [hep-ph]].
- [22] E. Arganda, M. J. Herrero, X. Marcano, R. Morales and A. Szyrkman, *Phys. Rev. D* **95**

- (2017) no.9, 095029 doi:10.1103/PhysRevD.95.095029 [arXiv:1612.09290 [hep-ph]].
- [23] T. T. Wang, S. M. Zhao, J. F. Zhang, X. X. Dong and T. F. Feng, Eur. Phys. J. C **82** (2022) no.7, 639 doi:10.1140/epjc/s10052-022-10613-5 [arXiv:2205.10485 [hep-ph]].
- [24] T. Moroi, Phys. Rev. D **53** (1996), 6565-6575 doi:10.1103/PhysRevD.53.6565 [arXiv:hep-ph/9512396 [hep-ph]].
- [25] F. Staub, Adv. High Energy Phys. **2015** (2015), 840780 doi:10.1155/2015/840780 [arXiv:1503.04200 [hep-ph]].
- [26] A. Flores-Tlalpa, J. M. Hernandez, G. Tavares-Velasco and J. J. Toscano, Phys. Rev. D **65** (2002), 073010 doi:10.1103/PhysRevD.65.073010 [arXiv:hep-ph/0112065 [hep-ph]].
- [27] R. L. Workman *et al.* [Particle Data Group], PTEP **2022** (2022), 083C01 doi:10.1093/ptep/ptac097.
- [28] A. Dedes, M. Paraskevas, J. Rosiek, K. Suxho and K. Tamvakis, JHEP **06** (2015), 151 doi:10.1007/JHEP06(2015)151 [arXiv:1504.00960 [hep-ph]].
- [29] J. Rosiek, Comput. Phys. Commun. **201**, 144-158 (2016) doi:10.1016/j.cpc.2015.12.011 [arXiv:1509.05030 [hep-ph]].
- [30] J. L. Yang, T. F. Feng, Y. L. Yan, W. Li, S. M. Zhao and H. B. Zhang, Phys. Rev. D **99** (2019) no.1, 015002 doi:10.1103/PhysRevD.99.015002 [arXiv:1812.03860 [hep-ph]].
- [31] X. X. Dong, S. M. Zhao, J. P. Huo, T. T. Wang and T. F. Feng, Phys. Rev. D **109**, no.5, 055019 (2024) doi:10.1103/PhysRevD.109.055019 [arXiv:2402.19131 [hep-ph]].
- [32] G. Aad *et al.* [ATLAS], Phys. Lett. B **796** (2019), 68-87 doi:10.1016/j.physletb.2019.07.016 [arXiv:1903.06248 [hep-ex]].
- [33] G. Cacciapaglia, C. Csaki, G. Marandella and A. Strumia, Phys. Rev. D **74** (2006), 033011 doi:10.1103/PhysRevD.74.033011 [arXiv:hep-ph/0604111 [hep-ph]].
- [34] M. Carena, A. Daleo, B. A. Dobrescu and T. M. P. Tait, Phys. Rev. D **70** (2004), 093009 doi:10.1103/PhysRevD.70.093009 [arXiv:hep-ph/0408098 [hep-ph]].
- [35] L. Basso, Adv. High Energy Phys. **2015** (2015), 980687 doi:10.1155/2015/980687 [arXiv:1504.05328 [hep-ph]].
- [36] F. Mahmoudi, JHEP **12** (2007), 026 doi:10.1088/1126-6708/2007/12/026 [arXiv:0710.3791 [hep-ph]].
- [37] K. A. Olive and L. Velasco-Sevilla, JHEP **05** (2008), 052 doi:10.1088/1126-6708/2008/05/052 [arXiv:0801.0428 [hep-ph]].

- [38] B. Abi *et al.* [Muon $g-2$], Phys. Rev. Lett. **126** (2021) no.14, 141801 doi:10.1103/PhysRevLett.126.141801 [arXiv:2104.03281 [hep-ex]].
- [39] A. M. Baldini *et al.* [MEG], Eur. Phys. J. C **76** (2016) no.8, 434 doi:10.1140/epjc/s10052-016-4271-x [arXiv:1605.05081 [hep-ex]].
- [40] A. Abdesselam *et al.* [Belle], JHEP **10** (2021), 19 doi:10.1007/JHEP10(2021)019 [arXiv:2103.12994 [hep-ex]].
- [41] G. Aad *et al.* [ATLAS], Phys. Rev. D **108** (2023), 032015 doi:10.1103/PhysRevD.108.032015 [arXiv:2204.10783 [hep-ex]].
- [42] G. Aad *et al.* [ATLAS], Phys. Rev. Lett. **127** (2022), 271801 doi:10.1103/PhysRevLett.127.271801 [arXiv:2105.12491 [hep-ex]].